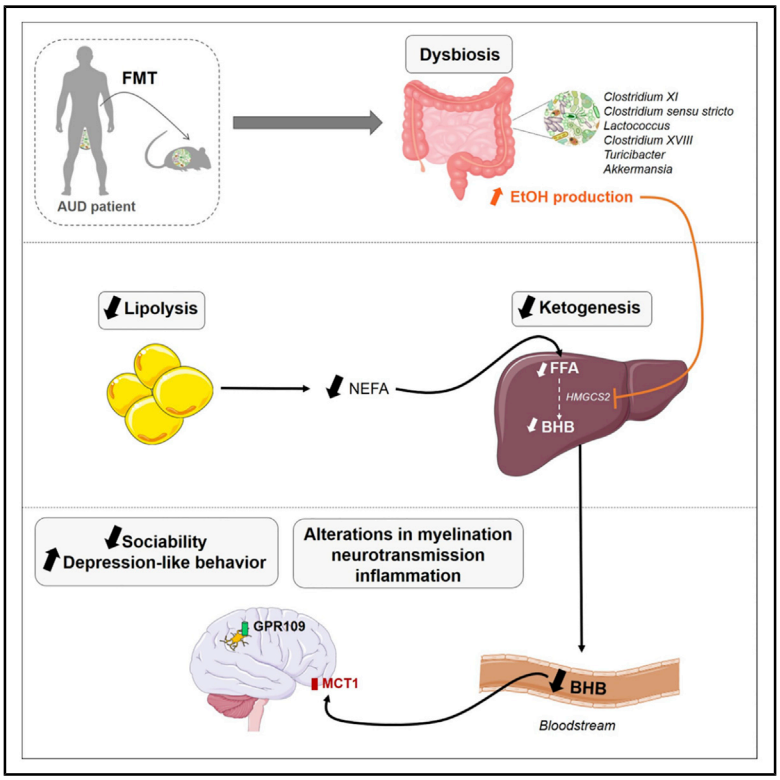
Cell Reports

Article

Gut Microbiota-Induced Changes in β-Hydroxybutyrate Metabolism Are Linked to Altered Sociability and Depression in Alcohol Use Disorder

Graphical Abstract



Highlights

- Gut alterations are related to impaired sociability in alcohol use disorder patients
- Human-to-mice microbiota transplantation reproduces metabolic and behavioral disorders
- Microbial ethanol production is linked to reduced β-hydroxybutyrate (BHB) synthesis
- In mice and humans, BHB level is associated with depression and social impairments

Authors

Sophie Leclercq, Tiphaine Le Roy, Sonia Furgiuele, ..., Peter Stärkel, Philippe de Timary, Nathalie M. Delzenne

Correspondence

philippe.detimary@uclouvain.be (P.d.T.), nathalie.delzenne@uclouvain.be (N.M.D.)

In Brief

Accumulating evidence highlights the importance of the gut-brain axis in alcohol use disorders. In this translational study, Leclercq et al. show that the transplantation of gut microbiota from alcoholic patients to mice induces metabolic disturbances impacting the adipose tissue and the liver, resulting in reduced β-hydroxybutyrate synthesis that drives neurobiological and behavioral alterations.

Leclercq et al., 2020, Cell Reports *33*, 108238
October 13, 2020 © 2020 The Author(s).
https://doi.org/10.1016/j.celrep.2020.108238

CellPress

Cell Reports

CellPress
OPEN ACCESS

Article

Gut Microbiota-Induced Changes in β-Hydroxybutyrate Metabolism Are Linked to Altered Sociability and Depression in Alcohol Use Disorder

Sophie Leclercq,[1,2] Tiphaine Le Roy,[2,3] Sonia Furgiuele,[4] Valentin Coste,[2] Laure B. Bindels,[2] Quentin Leyrolle,[2] Audrey M. Neyrinck,[2] Caroline Quoilin,[1] Camille Amadieu,[1,2] Géraldine Petit,[1] Laurence Dricot,[1] Vanessa Tagliatti,[4] Patrice D. Cani,[2,3] Kristin Verbeke,[5] Jean-Marie Colet,[4] Peter Stärkel,[6,7] Philippe de Timary,[1,8,9,*] and Nathalie M. Delzenne[2,9,10,*]

[1]Institute of Neuroscience, Université catholique de Louvain (UCLouvain), 1200 Brussels, Belgium
[2]Metabolism and Nutrition Research Group, Louvain Drug Research Institute, Université catholique de Louvain (UCLouvain), 1200 Brussels, Belgium
[3]WELBIO (Walloon Excellence in Life Sciences and Biotechnology), Louvain Drug Research Institute, Université catholique de Louvain (UCLouvain), 1200 Brussels, Belgium
[4]Laboratory of Human Biology & Toxicology, UMONS, 7000 Mons, Belgium
[5]Translational Research Center in Gastrointestinal Disorders, KU Leuven, 3000 Leuven, Belgium
[6]Laboratory of Hepato-Gastroenterology, Institute of Experimental and Clinical Research, Université catholique de Louvain (UCLouvain), 1200 Brussels, Belgium
[7]Department of Hepatogastroenterology, Cliniques Universitaires Saint-Luc, 1200 Brussels, Belgium
[8]Department of Adult Psychiatry, Cliniques Universitaires Saint-Luc, 1200 Brussels, Belgium
[9]These authors contributed equally
[10]Lead Contact
*Correspondence: philippe.detimary@uclouvain.be (P.d.T.), nathalie.delzenne@uclouvain.be (N.M.D.)
https://doi.org/10.1016/j.celrep.2020.108238

SUMMARY

Patients with alcohol use disorder (AUD) present with important emotional, cognitive, and social impairments. The gut microbiota has been recently shown to regulate brain functions and behavior but convincing evidence of its role in AUD is lacking. Here, we show that gut dysbiosis is associated with metabolic alterations that affect behavioral (depression, sociability) and neurobiological (myelination, neurotransmission, inflammation) processes involved in alcohol addiction. By transplanting the gut microbiota from AUD patients to mice, we point out that the production of ethanol by specific bacterial genera and the reduction of lipolysis are associated with a lower hepatic synthesis of β-hydroxybutyrate (BHB), which thereby prevents the neuroprotective effect of BHB. We confirm these results in detoxified AUD patients, in which we observe a persisting ethanol production in the feces as well as correlations among low plasma BHB levels and social impairments, depression, or brain white matter alterations.

INTRODUCTION

Alcohol use disorder (AUD) is a complex and widespread disease where pharmacotherapeutic options are still of limited efficacy (Jonas et al., 2014). Besides the role for neurotransmitters in the development of alcohol addiction (Gilpin and Koob, 2008), numerous studies suggests that disturbances of the brain functions in AUD is also due to alcohol-induced dysregulation of the neuroimmune system (Erickson et al., 2019). Indeed, activation of innate immune signaling and increased expression of pro-inflammatory cytokines occur in the brain of rodents chronically exposed to ethanol as well as in the brain of alcoholic patients (Blednov et al., 2012; He and Crews, 2008; Lippai et al., 2013; Pascual et al., 2015). Neuroinflammation could lead to demyelination (di Penta et al., 2013) and an altered balance between inhibitory and excitatory neurotransmissions (Olmos and Lladó, 2014) that also play a role in the regulation of alcohol drinking disorders.

In addition to the deleterious effects on the brain, chronic alcohol abuse also alters the composition and function of the gut microbiota (Bajaj, 2019; Bjørkhaug et al., 2019; Dubinkina et al., 2017; Leclercq et al., 2014; Mutlu et al., 2012; Peterson et al., 2017; Samuelson et al., 2019; Wang et al., 2018; Zhang et al., 2019). Microbial changes include, among others, a drastic decrease in *Faecalibacterium praustnizii*, a bacterium known for its anti-inflammatory properties (Sokol et al., 2008), and increased abundance of Lachnospiraceae (Firmicutes) (Bjørkhaug et al., 2019; Dubinkina et al., 2017; Leclercq et al., 2014). We have previously shown that leaky gut and microbial changes in AUD patients were correlated with the severity of

This is an open access article under the CC BY-NC-ND license (http://creativecommons.org/licenses/by-nc-nd/4.0/).

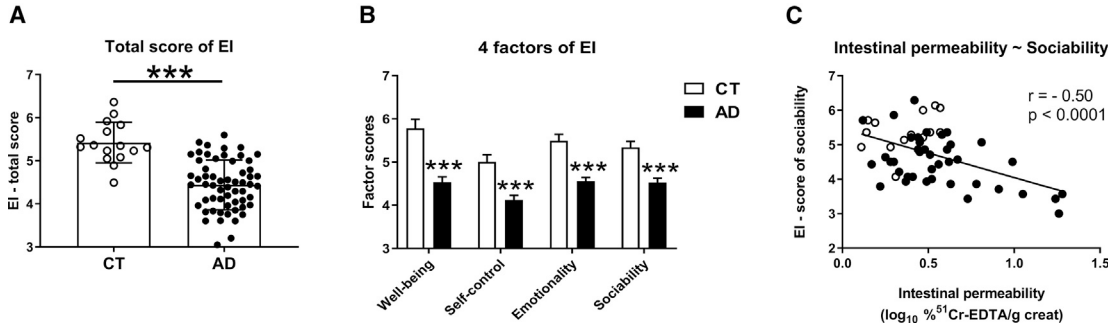


Figure 1. Sociability Is Correlated with Intestinal Permeability

Emotional intelligence (EI) was calculated, in AD patients (n = 59) and CT subjects (n = 16).

(A) Global trait EI score (mean ± SD).

(B) Four factors of EI (mean ± SEM).

(C) Correlation (Pearson's r) between the sociability scale of the EI and intestinal permeability (n = 57).

AD, alcohol-dependent (back dots); CTs, controls (white dots). ***p < 0.001 versus CT (unpaired t tests).

See also Table S1.

psychological symptoms such as depression, anxiety, and alcohol craving, suggesting a role for the gut microbiota in the development of alcohol addiction (Leclercq et al., 2014).

Since the gut microbiota is an important modulator of social behavior in rodents (Desbonnet et al., 2014; Gacias et al., 2016; Hsiao et al., 2013; Sherwin et al., 2019), we therefore explored, in the present study, the link between intestinal dysbiosis and different aspects of sociability in a cohort of AUD patients. The molecular mechanisms behind the gut microbiota-brain interactions were evaluated by using a preclinical model consisting of fecal microbiota transplantation (FMT) from AUD versus healthy subjects in mice, by using a metabolomics approach, and by evaluating the neuroactive impact of the modulation of a selected metabolite. We focused our experimental work on various addiction-associated behaviors (sociability, depressive- and anxiety-like behaviors and stress) and on key brain functions (myelination, neurotransmission, and inflammation). The preclinical studies we conducted meet the guidelines of Walter et al. (2020) for human microbiota-associated murine models to establish causal relationships between dysbiotic gut microbiomes and human diseases. Finally, a large cohort of AUD patients was used to test the relevance of the identified metabolite in the symptomatology of alcohol addiction.

RESULTS

Leaky Gut and Intestinal Dysbiosis Are Associated with Lower Sociability in Alcohol-Dependent Patients

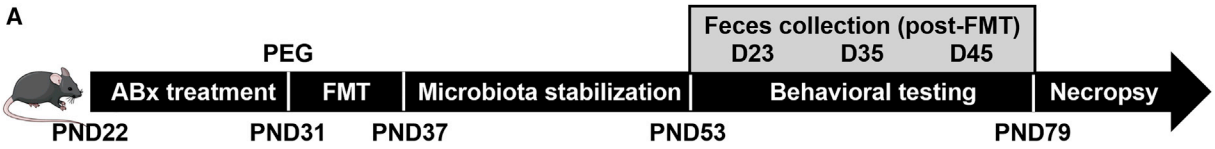
In this part of the study, we used data from our existing cohort of alcohol-dependent (AD) patients (selected according to DSM-IV criteria; Leclercq et al., 2014) to evaluate the relation between gut functions and sociability by using three different questionnaires. The trait emotional intelligence (EI) questionnaire (Mikolajczak et al., 2007; Petrides and Furnham, 2003) is a personality questionnaire constituted of four subfactors: well-being, self-control, emotionality, and sociability. Total EI and the four subfactors scores, were significantly reduced in AD patients compared to healthy subjects (control [CT]; Figures 1A and 1B). Interestingly, among the four subfactors, only the sociability subscale was significantly and negatively correlated with intestinal permeability, showing that subjects with a leaky gut had lower scores of sociability (Figure 1C; Table S1). These correlational results were confirmed with two other personality questionnaires, the D5D and the RSCS, where again only factors related to sociability, such as introversion and social anxiety, both positively correlated with intestinal permeability (Table S1).

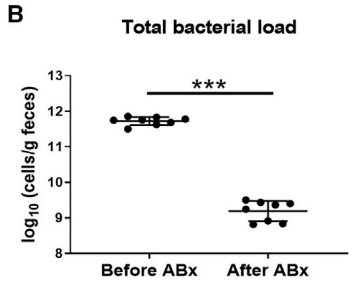
Hence, in addition to being correlated with scores of depression, anxiety and alcohol craving as shown in our previous study (Leclercq et al., 2014), we showed here that intestinal dysfunction is also associated with deficits in sociability, while difficulties in social interactions are known to play a major role in relapse (Zywiak et al., 2003). These observations led to postulate a role of the gut microbiota in the development of the psychological symptoms associated with alcohol dependence, including altered sociability. To assess this hypothesis, an FMT experiment was designed to study addiction-associated behaviors and underlying physiological and molecular alterations.

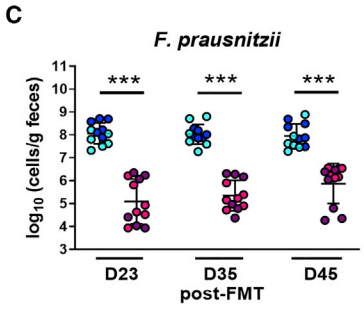
Microbial Transfer from Human Donors to Antibiotics-Treated Conventional Mice

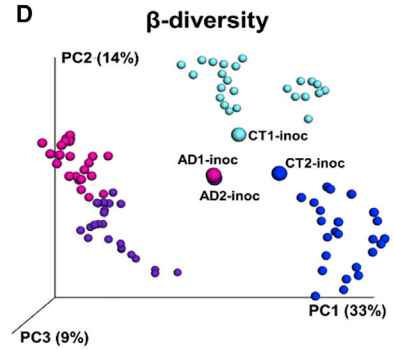
Three-week-old mice were treated with an antibiotic (ABx) cocktail for 10 days, followed by polyethylene glycol (PEG) in order to deplete the endogenous intestinal microbiota (Figure 2A). The efficacy of the ABx treatment was confirmed by showing a >250-fold reduction of bacterial DNA in the mice feces after ABx exposure (Figure 2B).

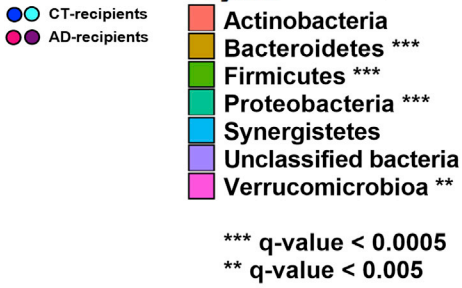
Two AD patients and two CT subjects were selected as human donors from a cohort of representative dysbiotic AD patients (Leclercq et al., 2014). The composition of gut microbiota was characterized and consisted mainly in lower bacterial count, lower abundance of *F. praustnizii*, and higher abundance of Lachnospiraceae in AD donors compared to CT (Figure S1). Other microbial characteristics of the human donors are displayed in Table S2. The AD donors were also selected based on biological features (leaky gut) (Figure S1; Table S2) and the severity of the psychological symptoms (high level of depression, anxiety, and

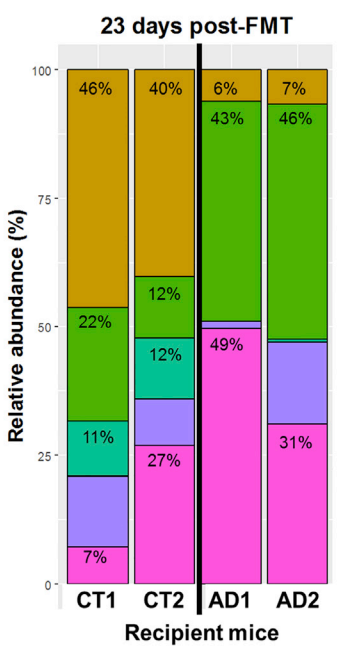


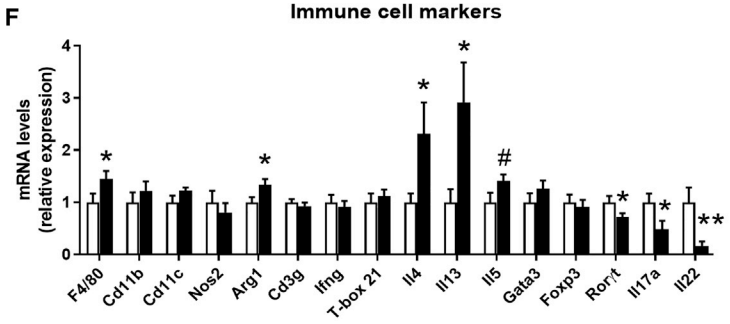


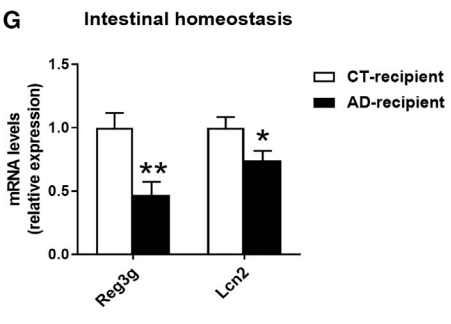


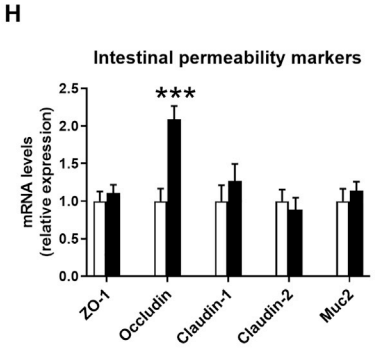


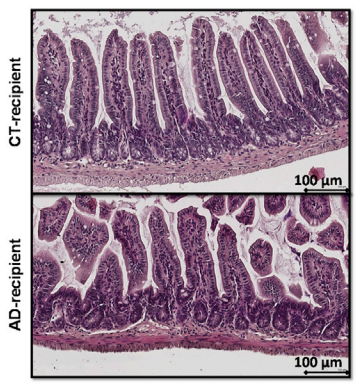


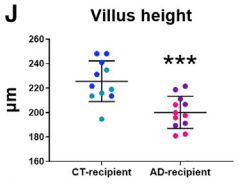


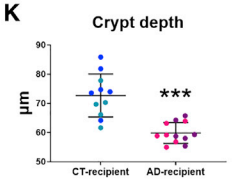












(legend on next page)

alcohol craving and low level of sociability) (Table S2). The fecal microbiota of these human donors were inoculated into mice, which were subsequently assessed for the successful and persistent bacterial engraftment. Since *F. prausnitzii* is present only in the human intestine (Nguyen et al., 2015), we first assessed by qPCR its levels in the feces of recipient mice. We found that *F. prausnitzii* was detectable in all mice and its levels were significantly reduced in AD-recipient mice, compared to CT-recipient mice, mimicking perfectly the differences observed in human donors (Figure 2C; Table S2). The difference in the level of *F. prausnitzii* between CT- and AD-recipient mice persisted up to 45 days after FMT (Figure 2C). Second, we performed 16S rRNA gene sequencing of mouse feces and caecal contents. The Shannon alpha-diversity index revealed that richness and evenness were significantly reduced in AD-recipient mice at all time points (Figure S2A) and the principal coordinate analysis (PCoA) based on Bray-Curtis and UniFrac metrics related to β-diversity showed a separation of CT- and AD-recipient samples along the first axis (Figures 2D and S2B, respectively). The PCoA plots also showed that the recipient mice clustered with their respective human donor, confirming that the microbial structures of the recipient mice were similar to their human inoculum. While the bacterial profile of each group of mice remained remarkably stable over time (Figure S2F), our analysis revealed drastic differences between the CT- and AD-recipient groups at all taxonomic levels (Figures S2F, S3, and S4). We observed that the total bacterial load (measured by qPCR) was reduced in AD-recipient mice, which is consistent with a lower bacterial count in AD humans (Figures S1B and S2C; Table S2). At the phylum level, we found decreased relative abundance of Bacteroidetes and increased Firmicutes in AD-recipient mice (Figure 2E). The relative abundance of Verrucomicrobia, and the level of *Akkermansia muciniphila*, were surprisingly higher compared to CT mice, with a high variation of its proportion between the donors within a group (Figures 2E and S2D). Abnormal expansion of *Akkermansia* following FMT has also been reported previously in germ-free mice (Le Roy et al., 2019; Sharon et al., 2019). This could be due to a lack of pressure exerted by the immune system on the intestinal microbiota (Zhang et al., 2015). In line with those previous observations, we found an overall attenuation of the markers of the defense immune mechanisms (alteration of Th2 and Th17 immune responses), associated with a loss of intestinal homeostasis (reduced expression of Reg3g and Lcn2), and modification of tight junction expression and atrophy of the mucosal structure in AD-recipient mice (reduced villus height and crypt depth in the ileum) (Figures 2F–2K). Finally, the Venn diagram indicated that 44% of the operational taxonomic units (OTUs) present in the CT inocula and 46% of the OTUs present in the AD inocula were successfully transferred to the CT- and AD-recipient mice, respectively (Figure S2E). All together, these results confirm the successful FMT procedure by using 3-week-old conventional mice treated with ABx and PEG as well as the persistence of the human microbiota engraftment up to 45 days after the transplantation. This model is therefore highly valuable and suitable to investigate gut-brain interactions in a physiological context and their consequences on behavior.

Mice Inoculated with AD Microbiota Exhibit Change in Behavior

To assess the impact of gut microbiota on social behavior, the three-chamber test was performed in CT- and AD-recipient mice. The test revealed that CT-recipient mice spent more time in the mouse chamber compared to the object chamber, while AD-recipient mice spent the same amount of time in the respective chambers. AD-recipient mice also spent more time in the object chamber compared to the CT-recipient mice (Figure 3A). Overall, these results showed a decreased social behavior in AD-recipient mice, as reflected by the sociability index (Figure 3B). We also found in AD-recipient mice that the latency to immobility in the forced swim test (FST) was lower, suggesting a more depressive-like behavior (Figure 3C), as well as higher corticosterone level, reflecting a higher stress level (Figure 3D). Results of the light/dark box and elevated-plus maze revealed no difference in anxiety-like behavior between AD- and CT-recipient mice (Figures 3E and 3F). In all tests, locomotor activity was similar for both groups of mice (Figures S5A–S5D). Altogether, these results showed that AD FMT in mice is sufficient to induce similar psychological features of AD patients in term of sociability, depression-like behavior, and stress level (cortisol level in Table S2). The molecular mechanisms underlying this relationship were investigated

Figure 2. Design of the FMT Experiment and Analysis of the Gut Microbiota and of Intestinal Immune System and Homeostasis of the Transplanted Mice

(A) Juvenile mice (PND22) were treated with a cocktail of ABx for 10 days, then with PEG before being inoculated with human microbiota of AD and CT donors. Behavioral testing started 22 days after the FMT and feces were collected 23, 35 and 45 days post-FMT.

(B) Quantification of the total bacterial load in the feces of mice before and after ABx treatment (n = 8, paired t test).

(C) Quantification of *F. prausnitzii* in the feces 23, 35 and 45 days post-FMT (n = 12 mice/group).

(D) PCoA plot of β-diversity using Bray-Curtis metrics (small dots represent mice feces collected 23, 35, and 45 post-FMT and cecal contents, large dots represent human CT- and AD-inoculum).

(E) Barplots showing the relative abundance of phyla in the feces of mice transplanted with the microbiota of healthy controls (CT1 and CT2) and of AD patients (AD1 and AD2) (n = 12 mice/group, Wilcoxon test, FDR-corrected p value).

(F and G) mRNA expression of markers involved in immunity and homeostasis in the ileum. AD-recipient mice are characterized by increased expression of M2 and Th2 markers (Arg1,Il4, Il13, Il5, and Gata3), no change in Th1 markers (Ifng and T-box 21) and Treg marker (Foxp3), reduced expression of Th17 markers (Rorγt, Il17a, and Il22) as well as altered intestinal homeostasis (Reg3g and Lcn2). n = 11–12 mice/group.

(H) mRNA expression of tight junctions in the ileum. n = 11–12 mice/group.

(I–K) Villi length and crypt depth with representative photomicrographs of hematoxylin and eosin stained ileum tissue.

n = 11–12 mice/group. Data represent mean ± SD (B, C, J, and K) and mean ± SEM (F–H). #p = 0.08; *p < 0.05; **p < 0.01; ***p < 0.001 versus CT-recipient mice, unpaired t tests unless otherwise specified. ABx, antibiotics; FMT, fecal microbiota transplantation; PND, postnatal day; inoc, inoculum.

See also Table S2 and Figures S1–S4.

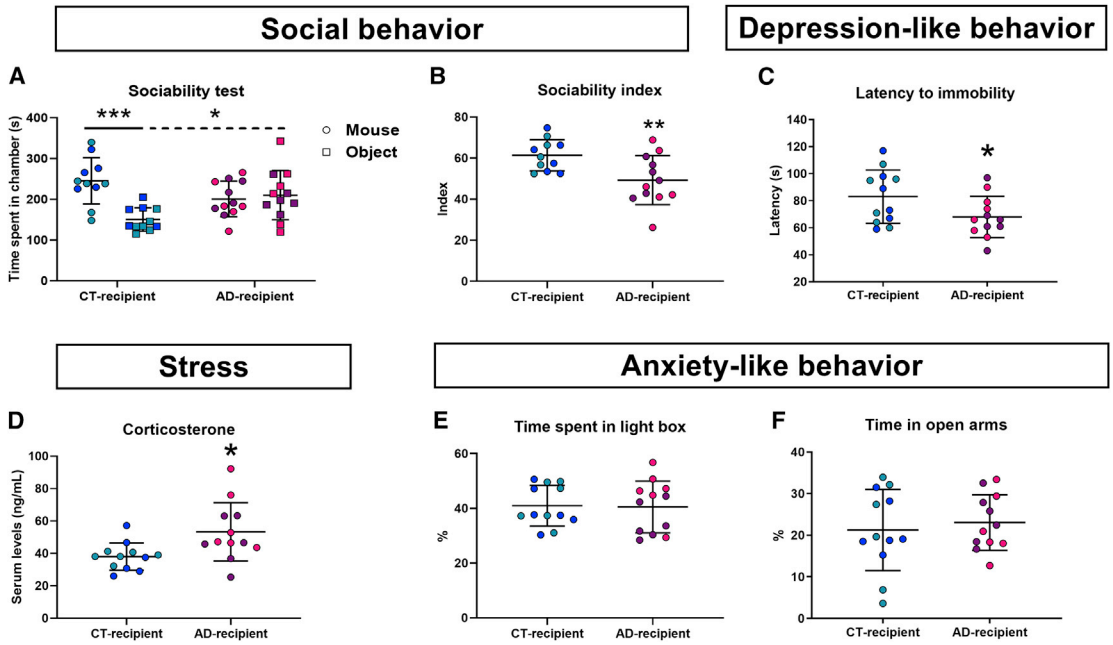


Figure 3. Impact of AD Microbiota on Behavior

(A and B) Social behavior and sociability index measured in the three-chamber sociability cage. n = 11–12 mice/group, two-way ANOVA followed by post hoc tests with Bonferroni correction.

(C) Depression-like behavior measured with the forced swim test.

(D) Stress level reflected by serum corticosterone concentration.

(E and F) Anxiety-like behavior measured with the light/dark box and the elevated-plus-maze.

For (C)–(F): n = 12 mice/group. Data represent mean ± SD. *p < 0.05; **p < 0.01; ***p < 0.001.

See also Figure S5.

in the brain and in peripheral metabolism to link these two distant phenomena.

Mice Inoculated with the AD Microbiota Exhibit Changes in Brain Functions

We collected two brain areas, the frontal cortex (FC) and the striatum (St), in order to investigate brain functions linked to myelination, neurotransmission, and inflammation that are all altered in AUD. We showed a downregulation of the expression of the myelin-related genes (Mobp and Mog) in the FC and in the St of AD-recipient mice (Figure 4A). Subunits α1 and α2 of gamma-aminobutyric acid ($GABA_A$) receptors (Gabra1 and Gabra2), $GABA_{B(1b)}$ receptor subunit (GabaBr1b), and N-methyl-D-aspartate (NMDA) receptor 2B (Grin2b) were upregulated in the FC of AD-recipient mice (Figure 4B). Quantification of neurotransmitters GABA and glutamate showed that only glutamate was reduced in the FC of AD-recipient mice (Figures 4C and 4D). This was associated with an increased protein expression of the post-synaptic density 95 (PSD-95), which plays a key role in regulating glutamatergic transmission and synaptic plasticity (Figures 4E and 4F). In addition, we found a significant upregulation of the mRNA expression of pro-inflammatory cytokines (Tnfa and Il1b) and chemokines (Cxcl15 and Ccl2) in the St of AD-recipient mice, while the FC did not show inflammatory markers. This local inflammatory response in the St was associated with elevated markers of microglial activation (Aif1, Cd68, and Nos2) including Gpr109a (Hcar2), the receptor for β-hydroxybutyrate (BHB), which was strongly correlated with that of pro-inflammatory cytokines ($r > 0.95$, $p < 0.001$; Figures 4G and S5H–S5K). A similar trend was observed for protein expression of striatal cytokines, although not reaching statistical significance, and correlated with the myelin-related gene Mog and with the sociability index (Figures S5E–S5G).

Taken together, these observations point toward disturbances of myelination, neurotransmission, and inflammation induced by AD microbiota transplantation that could negatively impact social behavior. We then investigated the metabolic pathways underlying gut-brain interactions.

AD Microbiota Reduces Lipolysis and Promotes Microbial Ethanol Production Resulting in Inhibition of Hepatic Ketogenesis and BHB Synthesis

The gut microbiota may communicate with the brain through different pathways, mainly neural, immune, or metabolic. Peripheral inflammation was rapidly discarded as a driver of central inflammation as none of the 10 different inflammatory cytokines and chemokines measured in the vena cava (reflecting systemic blood) were different between AD- and CT-recipient mice (Figure S5L). Consequently, we investigated peripheral metabolism via ^{1}H-NMR metabolomics analysis in the plasma. Partial least squares discriminant analysis (PLS-DA, supervised method) was applied to find discriminant metabolites between CT- and AD-

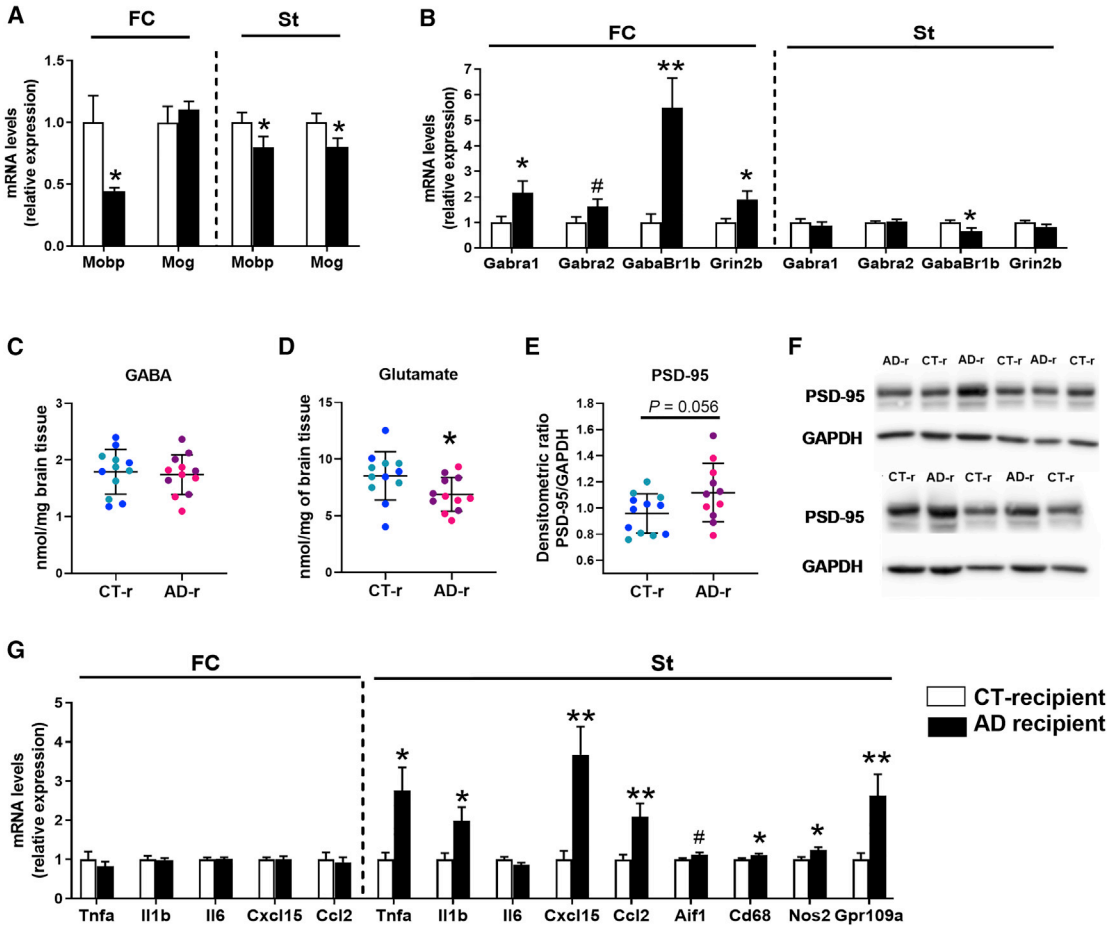


Figure 4. Alterations of Brain Functions in AD-Recipient Mice

(A) mRNA expression of myelin-related genes.

(B) mRNA expression of different subunits of $GABA_A$, $GABA_B$, and NMDA receptors.

(C and D) Quantification of GABA and glutamate in the frontal cortex.

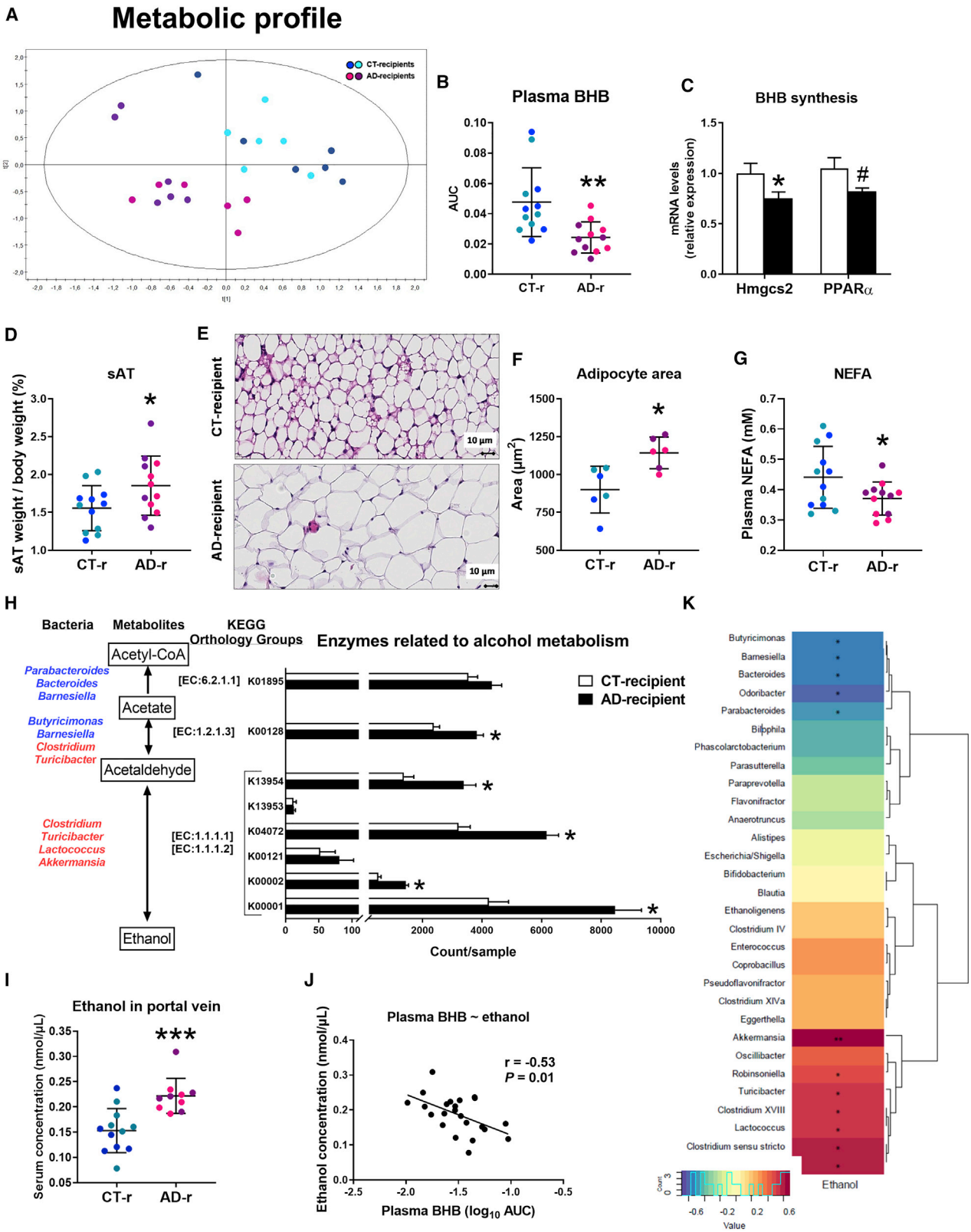
(E and F) Representative western blot of PSD-95 protein in the frontal cortex and quantification by densitometry normalized to the loading control GAPDH.

(G) mRNA expression of inflammatory cytokines, chemokines, and markers of microglial activation.

n = 12 mice/group, #p = 0.09; *p < 0.05; **p < 0.01 versus CT-recipient mice, unpaired t tests, mean ± SEM (or SD for (C)–(E). FC, frontal cortex; St, striatum. CT-r, control-recipient; AD-r, AD-recipient.

See also Figure S5.

recipient mice (Figure 5A). Interestingly, among those, levels of BHB were found to be lowered in AD-recipient mice (Figures 5B and S6A). BHB is a ketone body produced by the liver from fatty acids of the adipose tissue, released in the blood and used as energy substrate by neurons (Achanta and Rae, 2017). Primary regulators of hepatic ketogenesis include lipolysis of fatty acids from triacylglycerols, and transport of fatty acids from adipose tissue to the hepatocytes. Ketogenesis occurs in hepatic mitochondria where consecutive reactions catalyzed by multiple enzymes, including the 3-hydroxymethylglutaryl-CoA synthase (HMGCS2), lead to the conversion of beta-oxidation derived acetyl-CoA into acetoacetate, which is then reduced in BHB (Puchalska and Crawford, 2017). We therefore investigated the involvement of the liver and the adipose tissue, in the decrease in plasma BHB levels observed in AD-recipient mice. First, we found in AD-recipient mice a downregulation of hepatic expression of Hmgcs2, the main CT point of ketogenesis, and of transcription factor PPARα, its master regulator (Figure 5C). Second, we found that the subcutaneous adipose tissue (sAT) mass at necropsy was higher in AD-recipient mice (Figure 5D). Histological analysis revealed that the size of adipocytes was bigger in AD-recipient mice (Figures 5E and 5F), reflecting more lipid storage in the adipocytes and suggesting a decrease in lipolysis. Decreased plasma concentrations of non-esterified fatty acids (NEFAs), the primary substrates for hepatic ketogenesis, were also observed in AD-recipient mice (Figure 5G). Altogether, these results suggest that adipose tissue metabolism is changed in favor of triglycerides storage, thereby lowering blood NEFA levels and availability to hepatocytes, ultimately contributing to reduced liver ketogenesis and BHB synthesis. This is supported by negative correlation between NEFA and the weight of sAT, as well as positive correlation between NEFA and BHB (Figures S6B and S6C).



(legend on next page)

We then investigated whether and how the gut microbiota could be involved in the regulation of ketone bodies synthesis. We inferred functional profiles from taxonomic profiles obtained in cecal contents using PICRUSt, which revealed that pathways associated with alcohol metabolism were upregulated in AD-recipient mice (Figure 5H). Interestingly, ethanol is a major microbial product and has been shown to downregulate Hmgcs2 and PPARα (Deaciuc et al., 2004; Galli et al., 2001), indicating that ethanol may inhibit ketone bodies production. We therefore measured blood ethanol concentration in the portal vein and found that it was higher in AD-recipient mice, confirming higher ethanol production by the AD dysbiotic microbiota (Figure 5I). Furthermore, ethanol concentrations were negatively correlated with plasma BHB levels, supporting its inhibitory role on ketogenesis (Figure 5J). Consistent with higher portal vein ethanol level, the expression of ethanol-metabolizing enzymes (Adh1, Cyp2e1, and catalase) was upregulated in the liver of AD-recipient mice (Figure S6D). Finally, since ethanol is produced by the gut microbiota, we investigated which bacteria could be involved in alcohol metabolism by conducting correlational analysis. Portal vein ethanol level was positively correlated with the genera *Clostridium -sensu stricto, -XI, -XVIII*, *Lactococcus*, *Turicibacter*, and *Akkermansia*, which carry the genes coding for alcohol dehydrogenase [EC:1.1.1.1] and aldehyde dehydrogenase [EC:1.2.1.3], indicating that they have the functional ability to produce and/or metabolize ethanol. Among them, Clostridium genus has been recognized as an ethanol-producing bacteria (Wiegel et al., 2006). By contrast, the genera *Parabacteroides*, *Bacteroides*, *Barnesiella*, *Butyricimonas*, and *Odoribacter* were negatively correlated with ethanol levels. These bacteria express genes coding for the enzyme acetyl-CoA synthase [EC:6.2.1.1] which converts irreversibly acetate into acetyl-CoA (Figures 5H and 5K).

Altogether, these results suggest that AD microbiota transplantation reduced fatty acids lipolysis and increased microbial ethanol production. Consequently, the drop in NEFA availability, together with the inhibitory effect of ethanol on Hmgcs2, decreased liver ketogenesis and, subsequently, BHB synthesis and release in the systemic blood.

Modulation of BHB Levels Is Associated with Change in Social Behavior, Myelination, and Neuroinflammation

BHB is transported from the blood to the brain via the monocarboxylate transporter Mct1. In addition to its role as an energy substrate for neurons, BHB is also involved in many brain functions. We found an upregulation of the expression of Mct1 in the FC of AD-recipient mice (Figure S6E). Correlational analysis revealed that BHB was associated with markers of myelination (Mobp), neurotransmission (glutamate and GABA and NMDA receptors), neuroinflammation, and with sociability (Figures 6A–6C).

To challenge the role of BHB for brain dysfunction and reduction of social behavior, in a second experiment, we raised blood BHB levels by exposing mice for 6 weeks to a ketogenic diet (KD) (Figures 6D and 6E). Activation of liver ketogenesis was confirmed by enhanced expression of Hmgcs2 and PPARα, and of BHB brain transport by increased Mct1 expression (Figure 6F). Interestingly, social behavior and preference for social novelty were improved upon KD (Figures 6G and S6F). We then explored the effects of KD on brain functions. We found that myelin-related genes expression was increased in the KD group and correlated with sociability (Figures 6H and 6I). Conversely, expression of GABA and NMDA receptors were not impacted by KD except for an increase in GabraBr1b expression in the St (Figure 6J). The anti-inflammatory effect of KD was then assessed by measuring lipopolysaccharide (LPS)-induced cytokines and chemokines brain gene expressions. While the diet had no effect on the FC or St, we found a downregulation of Tnfα and Cxcl15 in the hippocampus (Figure 6K).

Overall, these results confirmed that BHB can take part in the regulation of social behavior and in neurobiological processes related to myelination and inflammation.

Confirming the Role of Altered Metabolic Pathways in Detoxified Human AD Patients: Microbial Ethanol Is Increased and Low BHB Is Associated with Social Impairments, Depression, and Lower Brain Myelination

In order to back-translate the experimental results into clinical practice, we collected biological, psychological, and

Figure 5. AD Microbiota Reduces Fatty Acids Lipolysis and Promotes Ethanol Production that Lead to Decreased Liver Ketogenesis and BHB Synthesis

(A) Score plot obtained after partial least squares discriminant analysis (PLS-DA) showing plasma metabolic profiles.

(B) Relative quantification of plasma BHB levels obtained by calculating the area under the curve of BHB peak in each metabolic spectrum.

(C) Liver mRNA expression of enzyme and transcription factor involved in ketogenesis and BHB synthesis.

(D) Weight of the subcutaneous adipose tissue (% of body weight) at necropsy.

(E and F) Representative histological pictures of subcutaneous adipose tissue and quantification of adipocyte area. n = 6 mice/group.

(G) Plasma concentration of non-esterified fatty acids.

(H) Representation of bacterial sequence count corresponding to Kyoto Encyclopedia of Genes and Genomes (KEGG) orthology groups related to alcohol metabolism, metabolites pathways, and potential bacteria involved in alcohol production and metabolism. Bacteria positively or negatively correlated with ethanol concentration measured in the portal vein are depicted in red and blue, respectively. Arrows pointing in both directions indicates that the bacterial enzymes are able to catalyze the reactions in both directions. $q < 0.05$ versus CT-recipient mice (FDR correction), unpaired t tests with Welch's correction.

(I) Ethanol concentration in the portal vein. n = 11 to 12 mice/group.

(J) Pearson's correlation between plasma BHB levels and ethanol concentrations measured in the portal vein.

(K) Heatmap showing positive (red) and negative (blue) correlations between bacteria and ethanol concentration measured in the portal vein. Significant correlations are marked with a star, $^{*}q < 0.05$; $^{**}q < 0.001$ (FDR correction).

For (B), (D), (F), (G), and (I): data represent mean ± SD. For (C) and (H): data represent mean ± SEM. n = 12 mice/group unless otherwise specified. Unpaired t tests, #p = 0.06; $^{*}p < 0.05$; $^{**}p < 0.01$; $^{***}p < 0.001$ versus CT-recipient mice.

See also Figure S6.

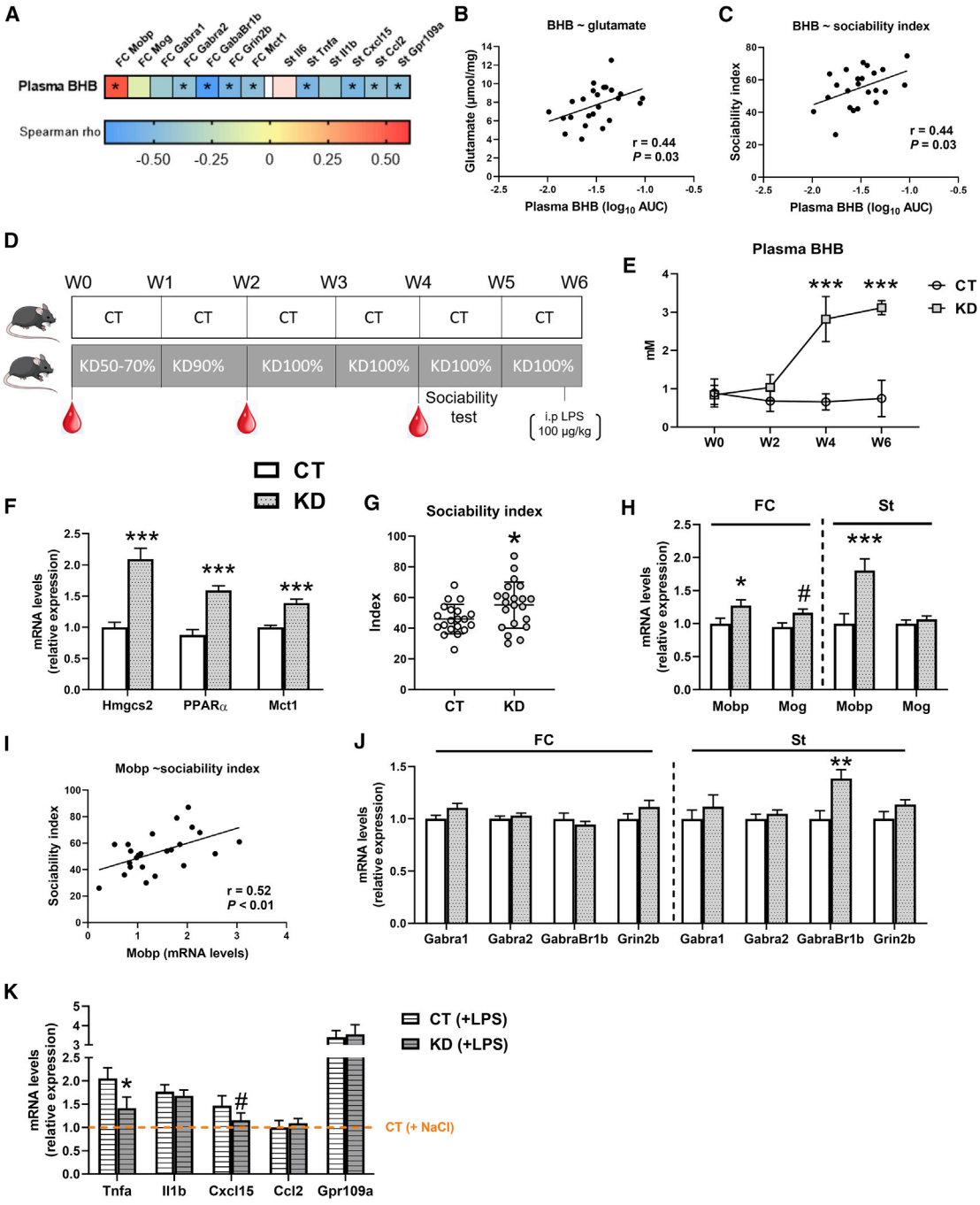


Figure 6. Ketogenic Diet (KD) Increases Blood Levels of β-Hydroxybutyrate, Improves Sociability, and Modulates Myelination and Neuroinflammation

(A) Heatmap of correlations between plasma BHB level and brain gene expression. Positive and negative correlations are depicted in red and blue, respectively. Significant ($p < 0.05$) correlations are marked with a star.

(B and C) Correlations (Pearson's r) between plasma BHB levels and glutamate quantified in the frontal cortex, and with the sociability index.

(D) Design of the KD experiment. Mice of the KD group (n = 21) were submitted to a keto-adaptation for 2 weeks, and then received 100% of the KD for 4 weeks. Control mice (CT, n = 21) received chow diet during the whole experiment. Blood samples were obtained before starting the KD, after 2 weeks and 4 weeks of exposure to the KD and at necropsy. For 9 KD and 9 CT mice, low dose LPS injection (intraperitoneally [i.p.]) has been performed 24 h before necropsy in order to study the anti-inflammatory effect of the diet.

(E) Kinetics of plasma levels of BHB during KD exposure. n = 9 mice/group.

(F) mRNA expression of enzyme and transcription factor regulating ketogenesis in the liver, and of BHB transporter in the frontal cortex. n = 12 mice/group.

(legend continued on next page)

neuroimaging data in several cohorts of AD patients to (1) measure the fecal and blood levels of ethanol, BHB, and NEFA, three key metabolic targets involved in the dialog between the gut microbiota, the adipose tissue, the liver, and the brain; (2) test the association between blood BHB levels and the psychological symptoms; and (3) test the potential involvement of BHB in brain myelination. In order to evaluate with no ambiguity the metabolic role of the microbiota, the FMT mice had not been exposed to alcohol. Consequently, we decided to test AD patients at the end of a 3-week detoxification program, thus allowing us to assess endogenous (microbial) ethanol production, without interference of external alcohol due to drinking. Since the portal vein is not accessible in humans without invasive surgery, the functional capacity of the gut microbiota to produce and/or metabolize ethanol was measured in feces. After three weeks of abstinence, ethanol was still detectable in 19 out of 20 AD patients, confirming ethanol production by intestinal microbes. Furthermore, fecal ethanol was higher in AD patients than CTs (Figure 7A). Second, we investigated the role of adipose tissue by measuring fat mass percentage by bioimpedance and NEFA plasma concentration. While we observed no fat mass difference between AD and healthy individuals (Figure 7B), we found a positive correlation between fat mass and intestinal permeability, suggesting that patients with leaky gut (and intestinal dysbiosis) had higher fat mass (Figure 7C). This is in accordance with our FMT model, where AD dysbiotic microbiota transplantation promoted the expansion of adipose tissue and reduced lipolysis. In addition, we observed a correlation between blood NEFA and BHB concentrations, also supporting that change in adiposity and NEFA levels influenced BHB synthesis (Figure 7D). Third, since in the transplanted mice, BHB was suggested to drive behavioral alterations, correlations between BHB and psychological symptoms were tested in AD patients. In a small cohort of 20 AD patients for which personality questionnaires were available, we found that BHB was positively associated with the score of EI and negatively associated with social anxiety (Figures 7E and 7F). Then, in larger cohorts of AD patients (n = 62 to 90), we found that BHB was negatively correlated with the scores of depression and alcohol craving (Figures 7G and 7H). These correlations suggest that recently detoxified AD patients with lower levels of BHB have lower social abilities and higher levels of depression and craving. Finally, to test the implication of BHB in myelination, we conducted a small pilot MRI study (3D T1 and Diffusion Tension Imaging) on 22 AD patients in order to extract the fractional anisotropy (FA) maps. FA is often used to assess white matter integrity, which can be impacted by various parameters including myelination. Interestingly, we found that plasma BHB levels positively correlated with the FA in two areas of the white matter, the forceps major (FM) and the left superior longitudinal fasciculus (LSLF) (Figures 7I–7K). Although preliminary, these correlations obtained in AD patients are consistent with the involvement of BHB in brain myelination.

DISCUSSION

Intestinal permeability and gut microbiota alterations have been previously associated with psychological symptoms of alcohol dependence including depression, anxiety, and alcohol craving (Leclercq et al., 2014). Social deficits are also essential features of AUD patients, and are related to difficulties in interpreting the emotions of others, sensitivity to social rejection (Maurage et al., 2012), and difficulties in taking into account the perspectives of others (Maurage et al., 2015), which results in high rates of relapses after alcohol withdrawal (Zywiak et al., 2003). Consistent with that, we found that AUD patients scored specifically lower than healthy CTs on social abilities as reported with various personality questionnaires. Interestingly, while the link between gut microbiome and social behavior has been demonstrated in multiple animal models (Sherwin et al., 2019), our clinical data report a link between leaky gut and social impairments in humans.

Consequently, we used a FMT model from AUD patients to mice in order to unravel the metabolic and neurobiological mechanisms associated with emotional and social behaviors related to alcohol addiction. FMT has been successfully used to demonstrate a causal relationship among intestinal microbiota and several diseases, such as obesity (Ridaura et al., 2013), irritable bowel syndrome (De Palma et al., 2017), autism (Sharon et al., 2019), and depression (Zheng et al., 2016). FMT from human to mice is often performed in GF mice but these initially present with significant modifications of behavior including sociability (Desbonnet et al., 2014; Diaz Heijtz et al., 2011; Neufeld et al., 2011). To overcome these difficulties, we used a valid alternative to GF mice which consists in conventional juvenile mice subjected to initial microbiota depletion with broad-spectrum ABx and PEG (Le Roy et al., 2019; Wrzosek et al., 2018) followed by the inoculation of a well-characterized fecal microbiota coming from AUD patients and healthy subjects. Although the FMT from human to mice was not 100% efficient due, for instance, to abnormal overgrowth of some bacteria belonging to Verrucomicrobia, β-diversity indices clearly showed that CT-recipient mice clustered separately from the AD-recipient mice, and that each group of recipient mice clustered with its respective human donor. Furthermore, the drastic decrease in Bacteroidetes and in *F. prausnitzii* associated with an increased abundance of Lachnospiraceae, which are important features of the human alcoholic microbiota (Bjørkhaug et al., 2019; Dubinkina et al., 2017;

(G) Social behavior assessed in the 3-chamber apparatus. n = 21/group.
(H) mRNA expression of myelin-related genes in the frontal cortex and striatum, n = 12 mice/group.
(I) Correlations (Pearson's r) between myelin-related gene and sociability index.
(J) mRNA expression of GABA and NMDA receptors measured in the frontal cortex and striatum. n = 12 mice/group.
(K) mRNA expression of LPS-induced inflammatory cytokines and chemokines measured in the hippocampus. n = 9 mice/group. Orange line represents the mRNA expression in CT mice (n = 6) injected with NaCl.
For (E) and (G): data represent mean ± SD. For (F), (H), (J), and (K): data represent mean ± SEM. Unpaired t tests, #$p < 0.10$; *$p < 0.05$; ***$p < 0.001$ versus CT-recipient mice. BHB, β-hydroxybutyrate; KD, ketogenic diet; FC, frontal cortex; St, striatum.
See also Figure S6.

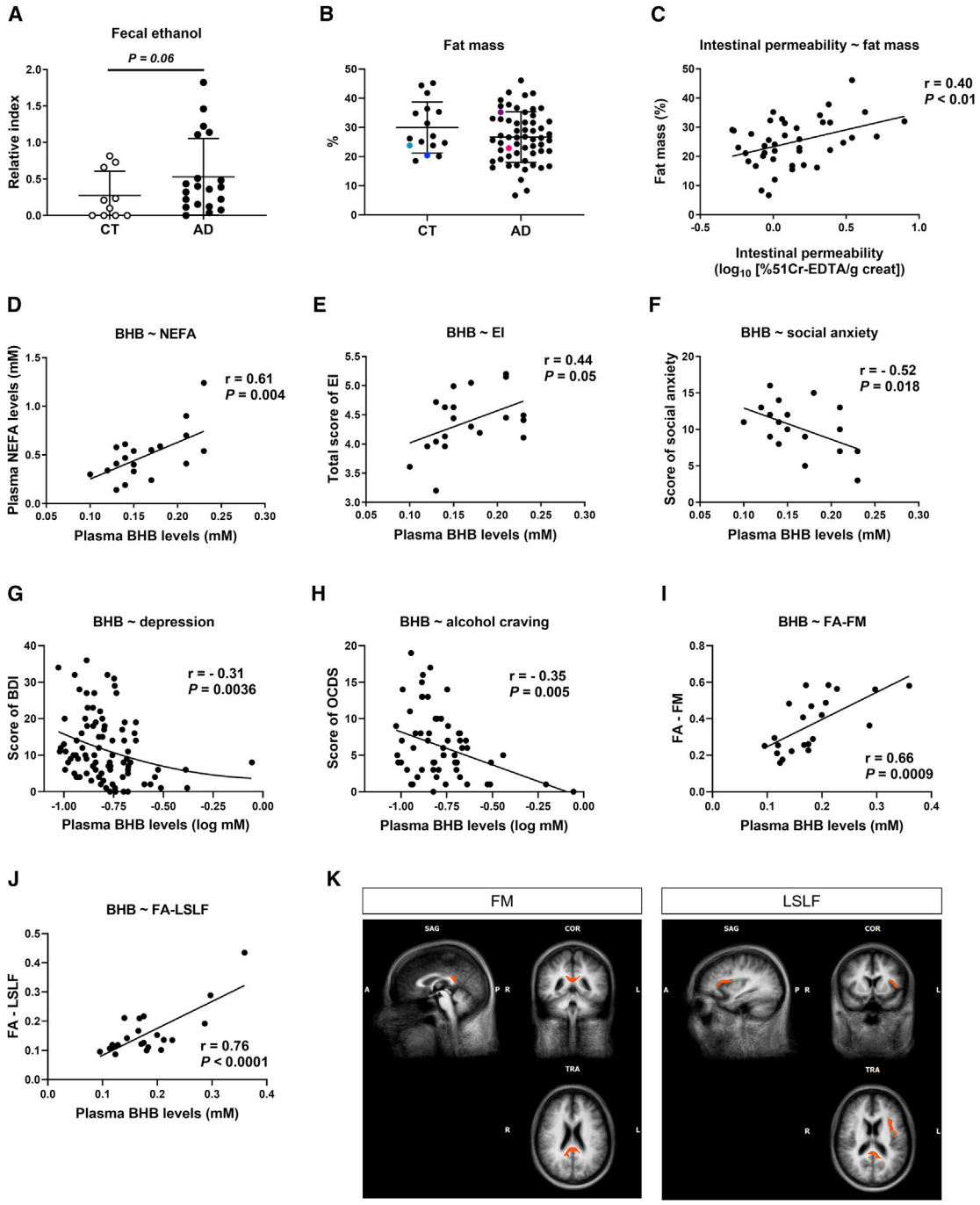


Figure 7. Microbial Ethanol Is Increased in Detoxified AD Patients and β-Hydroxybutyrate Is Correlated with the Psychological Symptoms and Brain Myelination

(A) Fecal ethanol levels in detoxified AD patients (n = 20) and controls (n = 10), Mann-Whitney test, mean ± SD.

(B) Measurement of fat mass percentage by bioimpedance, n = 16 CT and 58 AD subjects. Subjects used for FMT experiment are colored, mean ± SD.

(C) Correlation (Pearson's r) between intestinal permeability and fat mass percentage in AD patients (n = 41).

(D–H) Correlation (Pearson's r) between plasma BHB and NEFA in AD patients (n = 20), the total score of EI (n = 20), the score of social anxiety (n = 20), the score of depression (n = 90), and the score of alcohol craving (n = 62).

(I–K) Correlation maps between subject's FA normalized maps and BHB values, corrected using Monte Carlo simulation. Clusters in the forceps major and in the left superior longitudinal fasciculus are represented (n = 22 AD patients).

AD, alcohol-dependent; BHB, β-hydroxybutyrate; CT, healthy controls; FA, fractional anisotropy; NEFA, non-esterified fatty acids.

Leclercq et al., 2014; Mutlu et al., 2012), were perfectly reproduced in the transplanted mice.

Overall, our FMT experiment revealed that mice transplanted with the feces of AUD patients exhibited reduced sociability, increased depression-like behavior, and stress levels. These behavioral alterations were associated with brain function disturbances including myelination, neurotransmission, and neuroinflammation. Metabolomics analysis revealed that increased microbial ethanol production and reduction of adipose tissue lipolysis, leading to decreased release of NEFA in the circulation, result in inhibition of liver ketogenesis and reduction of BHB synthesis in mice inoculated with AD microbiota. Knowing the multiple neuroprotective effects of BHB, we postulated that the reduction of hepatic ketogenesis and BHB synthesis is at the origin of brain dysfunction in AD-recipient mice. Obviously, the low number of human donors (n = 2 AUD patients and 2 healthy subjects), even though the selected patients were representative of a group of dysbiotic AD patients, constitutes a limitation of the present study. However, recently, a replication study has been conducted by an independent group showing that FMT from AUD patients also leads to increased depression-like behavior and reduced sociability in mice although mechanisms linking gut dysbiosis and altered behavior have not been investigated by those authors (Zhao et al., 2020). Furthermore, our FMT study responds to the recommendations and guidelines for human microbiota-associated rodent models (Walter et al., 2020), and the mechanistic findings highlighting a role for the gut-liver-brain axis obtained in this preclinical model have to be considered not as an end-point per se, but rather as a proof of concept that is eventually confirmed by various measurements in biological samples issued from larger AUD patient cohorts.

First, we tried to elucidate the mechanisms linking AD microbiota inoculation to changes in behavior and brain functions. While several pathways, mainly neural, metabolic or immune ones, have been suggested to drive gut-brain interactions (Cryan and Dinan, 2012; Forsythe et al., 2016), we confirmed that the disturbances observed in our study were not induced by a peripheral inflammatory response, but rather related to blood metabolites changes. Indeed, we found that portal ethanol was increased, while systemic BHB and NEFA were decreased in AD-recipient mice. Intestinal microbiota is a major source of endogenous ethanol (Sarkola and Eriksson, 2001; Yuan et al., 2019). Since mice were not exposed to alcohol during experiments, increased portal vein ethanol concentration strongly suggests a higher colonization of the AD microbiota by alcohol-producing bacteria, such as for instance *Clostridium*, *Lactococcus*, *Turicibacter*, and *Akkermansia*, which all have the functional ability to produce and or metabolize ethanol. This is in accordance with a metagenomic study that noticed that AUD patients gut microbiome is enriched in functions related to alcohol metabolism (Dubinkina et al., 2017). Interestingly, abstinent AUD patients still presented with higher ethanol level in their feces, confirming ethanol production by intestinal microbes. We therefore hypothesize that this small but chronic endogenous production of ethanol by gut microbes induces changes in liver metabolism, and particularly an inhibition of the ketogenesis pathway. BHB is a ketone body produced by the liver from acetyl-CoA, which in turn comes from the oxidation of fatty acids (Mattson et al., 2018). The main control point of ketogenesis is the liver mitochondrial enzyme Hmgsc2, which is under the control of PPARα (Grabacka et al., 2016)—both of which are inhibited by ethanol (Deaciuc et al., 2004; Galli et al., 2001), and were downregulated in our AD-recipient mice. In addition, we found that adipose tissue metabolism of AD-recipient mice was shifted toward triglyceride storage, decreasing the availability of NEFA for liver ketogenesis—both of which contributed to reduced blood BHB. Data obtained in AUD patients support the existence of a similar mechanism in humans: blood NEFA concentrations were positively correlated with BHB levels and interestingly, adiposity was correlated with intestinal permeability, suggesting a link between fat mass and leaky gut. This corroborates mice data showing that AD microbiota transplantation promotes the expansion of adipose tissue. Altogether, experimental and clinical data support the concept that the gut microbiota could interfere with the metabolism of both the adipose tissue and the liver, with a consequent decrease in the availability of BHB, potentially affecting brain functions and behavior.

While glucose is the main energy substrate for the brain, monocarboxylic acids (ketone bodies, acetate, lactate) are vital alternative energy sources for neurons (Puchalska and Crawford, 2017). In our study, the expression of monocarboxylate transporter Mct1 was increased in AD-recipient mice, which might reflect a metabolic adaptation necessary to fuel brain cell functions in the case of neuroinflammation (Moreira et al., 2009). Interestingly, the reduction of BHB in alcoholics undergoing detoxification was postulated several decades ago to lead to brain energy depletion and contribute to alcohol withdrawal symptoms and neurotoxicity (Derr et al., 1983). Consistent with that, we hypothesize that the decrease in BHB levels observed in AD-recipient mice shifts the brain to a state of energy depletion that might contribute to demyelination, dysregulation of the GABA/glutamate balance, and neuroinflammation. This hypothesis is supported by the multiple neuroprotective effects of BHB. It is a precursor of membrane lipids in brain cells and involved in the myelination process (Koper et al., 1981; Webber and Edmond, 1979). It exerts anticonvulsant effects likely through the modulation of GABA and glutamate pathways (McNally and Hartman, 2012), and has anti-inflammatory properties through its receptor GPR109A (Fu et al., 2015; Puchalska and Crawford, 2017; Rahman et al., 2014). In the present study, AD-recipient mice exhibited brain downregulation of myelin-related genes, which has also been shown post-mortem in human brains of alcoholics (Lewohl et al., 2000). Our preliminary neuroimaging data showed in AUD patients a correlation between plasma BHB levels and FA measures in the FM, a white matter fiber bundle part of the corpus callosum, and in the LSLF. FA can be influenced by different parameters including axonal density and diameter, myelination, or inflammation. In the mouse brain, FA correlates positively with the myelin basic protein, a marker for myelination (Chang et al., 2017), and it has been shown in AUD patients that reduced FA in the corpus callosum was compatible with sustained demyelination and glial immune reaction (De Santis et al., 2019). Furthermore, a mouse model of demyelination showed that feeding mice a KD robustly increased the remyelination in the corpus callosum (Stumpf et al., 2019). Evidence

for major white matter microstructure disruption in the corpus callosum and the LSLF has previously been provided in AUD patients and reduced FA values in those regions were functionally associated to deficits in neuropsychological performances (Pfefferbaum et al., 2006, 2009; Yeh et al., 2009). Taken together, these and our data reinforce the involvement of BHB in the myelination process. A link between myelination, depression-like, and social behaviors has already been described in rodents (Liu et al., 2012, 2016) and was suggested to be mediated by bacterial metabolites (Gacias et al., 2016). Interestingly, our human data showed that lower plasma BHB levels in AD patients were associated with higher psychological distress, including social impairments, depression, and alcohol craving. This is consistent with the results of our FMT experiment showing that AD microbiota transplantation induced depression-like behavior and reduced social behavior in mice. The link we observed among microbiota, BHB levels, and alcohol craving in AD patients would certainly deserve further investigation. However, in this FMT study, alcohol-drinking behaviors have not been tested for an obvious reason: the goal was to investigate the effect of AD microbiota itself on behavior, brain functions, and metabolism, without the interference of ethanol. Not exposing mice to ethanol in the current study allowed us to ascertain that the effects of the microbiota on liver, brain, and behavior were direct. Nevertheless, the AD microbiota transplantation induced brain changes that have previously been shown to be related to alcohol drinking behavior. First, we found an upregulation of GABA and NMDA receptors in the FC of AD-recipient mice associated with a decrease in glutamate and increase in PSD-95. Alterations in the excitatory (glutamatergic) and the inhibitory (GABAergic) neurotransmitter systems have been previously related to withdrawal symptoms, emotion enhancement, response to stress, and drinking motivation and might hence play a role in addiction development (Gilpin and Koob, 2008; Herman et al., 2004). The role of PSD-95 might also be important since mice knocked out (KO) for PSD-95 exhibit reduced ethanol consumption (Camp et al., 2011). Of note, other neurotransmitters that play a role in alcohol drinking behavior and that can be influenced by the gut microbiota, such as the dopaminergic system (Jadhav et al., 2018), have not been investigated in this present study. Second, we found increased inflammation and markers of activated microglia in the St of AD-recipient mice. The role of striatal immune reactions for reward processes and alcohol-seeking behaviors (Chen et al., 2011) is supported by rodent studies where voluntary ethanol consumption was induced by a targeted neuro-immune response (Blednov et al., 2012; Valenta and Gonzales, 2016). Altogether, this suggests that AD microbiota transplantation might enhance alcohol-seeking behavior. Testing the effect of AD microbiota transplantation on drinking behavior, and reversely testing the metabolic impact of ethanol in FMT animals, are important issues that would enhance our understanding of the role of the microbiota. Based on the evidence we bring on the sufficient role of the microbiota alone, these hypotheses would deserve experimental confrontations. Finally, to support the role of BHB in the modulation of behavior and brain functions, we successfully increased the systemic BHB level in mice through exposure to a KD and observed an improvement of sociability, associated with increased myelination markers and reduced neuroinflammation. Although we cannot ascertain that the beneficial impact of KD is directly due to BHB and not to other nutrients present in the diet, a recent study showed that KD attenuates the symptoms of alcohol withdrawal in rats (Dencker et al., 2018). This encourages testing clinically the effect of BHB in AUD patients.

In conclusion, we found that the transplantation of human AD microbiota to mice recapitulated some behavioral alterations associated with alcohol dependence, including reduced sociability, increased depression-like behavior, and higher stress level. Thanks to FMT which makes the investigation of the brain possible, we found that behavioral alterations were associated with decreased myelination, unbalanced GABA/glutamate neurotransmission, and neuroinflammation. The inoculation of a dysbiotic AD microbiota coming from a specific subset of AD patients led to a reduced synthesis of BHB that could be at the origin of the alterations in brain functions and behavior in mice. The metabolic origin of BHB levels perturbation seems to lie in the functional capacity of AD microbiota to produce ethanol and to alter adipose tissue and liver metabolism. In abstinent alcoholics, ethanol was still produced by the intestinal microbiota and low BHB levels were correlated with psychological distress including social impairments, depression, and alcohol craving, which constitute important factors of relapse. Altogether, these results suggest that nutritional therapies, aiming at restoring the gut microbiota (i.e., via prebiotics supplementation) or ketone body metabolism, might be beneficial on the gut-liver-brain axis and decrease the risk of relapse in AUD patients.

STAR★METHODS

Detailed methods are provided in the online version of this paper and include the following:

- KEY RESOURCES TABLE
- RESOURCE AVAILABILITY
  - Lead Contact
  - Materials Availability
  - Data and Code Availability
- EXPERIMENTAL MODEL AND SUBJECT DETAILS
  - For human studies
  - For in vivo animal studies
- METHOD DETAILS
  - Psychological questionnaires
  - Intestinal permeability and gut microbiota composition measurements in humans
  - Ethanol measurement in human fecal samples by GC/MS
  - Neuroimaging assessment
  - Antibiotic treatment and bowel cleansing procedure
  - Inoculum preparation
  - Human microbiota transplantation into conventional mice
  - Gut microbiota analysis
  - Metabolic profiling by ^{1}H-NMR spectroscopy
  - Behavioral testing
  - Blood and tissue sampling
  - RNA extraction and RT-qPCR analysis

- Protein extraction and western blot analysis
- Cytokines, corticosterone and ethanol assays
- GABA and glutamate ELISA
- Beta-hydroxybutyrate and non-esterified fatty acids assays

● QUANTIFICATION AND STATISTICAL ANALYSIS

SUPPLEMENTAL INFORMATION

Supplemental Information can be found online at https://doi.org/10.1016/j.celrep.2020.108238.

ACKNOWLEDGMENTS

We thank Prof. Jean-François Collet for the access to anaerobic chamber, Karen-Ann Neufeld for her tips regarding the corticosterone assay, Greg Stanisz for his advice for the neurotransmitters assay, Rose-Marie Gobbels for histological preparations, and the technicians (Bouazza Es Saadi, Isabelle Blave, and Véronique Allaeys) for their excellent technical help. Finally, we warmly thank Dr. Jonathan van Eyll for his careful reading and comments that improved the manuscript. S.L. was a post-doc fellow funded by the Belgium National Scientific Research Fund (FRS-FNRS) and now by UCLouvain (Action de Recherche Concertée ARC18-23/092). C.Q. is a post-doc fellow funded by FRS-FNRS. P.D.C. is a senior research associate at FRS-FNRS and supported by the Funds Baillet Latour (Grant for Medical Research 2015). T.L.R. was a post-doc fellow funded by FRFS-WELBIO (WELBIO-CR-2017C-02). P.d.T. is supported by Fonds de Recherche Clinique of Secteur Santé de l'UCLouvain. N.M.D. is a recipient of grants from Wallonia (FiberTAG project from the European Joint Programming Initiative "A Healthy Diet for a Healthy Life"), from FRS-FNRS (PINT-MULTI R.8013.19 [NEURON, call 2019] and PDR T.0068.19). The bioprofiling platform was supported by the European Regional Development Fund and the Walloon Region, Belgium.

AUTHOR CONTRIBUTIONS

S.L., N.M.D., and P.d.T. designed the study; T.L.R. designed the FMT protocol; S.L., V.C., and Q.L. performed experiments; S.L., V.C., and C.Q. analyzed the data; S.F., V.T., J.-M.C., and K.V. performed metabolomics profiling; S.L. and L.B.B. performed 16S metagenomics and PICRUSt analysis; G.P. and L.D. provided biological samples and MRI data; S.L. and C.A. performed statistical analysis; A.M.N. helped with animal experiments; T.L.R., L.B.B., A.N.M., C.Q., P.D.C., and P.S. helped with data interpretation; S.L., N.M.D., and P.d.T. wrote the paper; N.M.D. and P.d.T. supervised the project; and all authors provided support and constructive criticism throughout the project and approved the final version of the paper.

DECLARATION OF INTERESTS

P.D.C. is the inventor of patent applications dealing with the use of *A. muciniphila* and its components in the context of obesity and related disorders. P.D.C. is co-founder of A-Mansia Biotech SA. The other authors declare no competing interests.

Received: September 20, 2019
Revised: August 4, 2020
Accepted: September 16, 2020
Published: October 13, 2020

REFERENCES

Achanta, L.B., and Rae, C.D. (2017). β-Hydroxybutyrate in the brain: one molecule, multiple mechanisms. Neurochem. Res. *42*, 35–49.

Bajaj, J.S. (2019). Alcohol, liver disease and the gut microbiota. Nat. Rev. Gastroenterol. Hepatol. *16*, 235–246.

Bindels, L.B., Neyrinck, A.M., Claus, S.P., Le Roy, C.I., Grangette, C., Pot, B., Martinez, I., Walter, J., Cani, P.D., and Delzenne, N.M. (2016). Synbiotic approach restores intestinal homeostasis and prolongs survival in leukaemic mice with cachexia. ISME J. *10*, 1456–1470.

Bjørkhaug, S.T., Aanes, H., Neupane, S.P., Bramness, J.G., Malvik, S., Henriksen, C., Skar, V., Medhus, A.W., and Valeur, J. (2019). Characterization of gut microbiota composition and functions in patients with chronic alcohol overconsumption. Gut Microbes *10*, 663–675.

Blednov, Y.A., Ponomarev, I., Geil, C., Bergeson, S., Koob, G.F., and Harris, R.A. (2012). Neuroimmune regulation of alcohol consumption: behavioral validation of genes obtained from genomic studies. Addict. Biol. *17*, 108–120.

Bourin, M., and Hascoët, M. (2003). The mouse light/dark box test. Eur. J. Pharmacol. *463*, 55–65.

Camp, M.C., Feyder, M., Ihne, J., Palachick, B., Hurd, B., Karlsson, R.-M., Noronha, B., Chen, Y.-C., Coba, M.P., Grant, S.G., and Holmes, A. (2011). A novel role for PSD-95 in mediating ethanol intoxication, drinking and place preference. Addict. Biol. *16*, 428–439.

Can, A., Dao, D.T., Arad, M., Terrillion, C.E., Piantadosi, S.C., and Gould, T.D. (2011). The mouse forced swim test. J. Vis. Exp. *59*, e3638.

Chang, E.H., Argyelan, M., Aggarwal, M., Chandon, T.S.S., Karlsgodt, K.H., Mori, S., and Malhotra, A.K. (2017). The role of myelination in measures of white matter integrity: combination of diffusion tensor imaging and two-photon microscopy of CLARITY intact brains. Neuroimage *147*, 253–261.

Chen, G., Cuzon Carlson, V.C., Wang, J., Beck, A., Heinz, A., Ron, D., Lovinger, D.M., and Buck, K.J. (2011). Striatal involvement in human alcoholism and alcohol consumption, and withdrawal in animal models. Alcohol. Clin. Exp. Res. *35*, 1739–1748.

Cole, J.R., Wang, Q., Fish, J.A., Chai, B., McGarrell, D.M., Sun, Y., Brown, C.T., Porras-Alfaro, A., Kuske, C.R., and Tiedje, J.M. (2014). Ribosomal Database Project: data and tools for high throughput rRNA analysis. Nucleic Acids Res. *42*, D633–D642.

Couch, Y., Trofimov, A., Markova, N., Nikolenko, V., Steinbusch, H.W., Chekhonin, V., Schroeter, C., Lesch, K.-P., Anthony, D.C., and Strekalova, T. (2016). Low-dose lipopolysaccharide (LPS) inhibits aggressive and augments depressive behaviours in a chronic mild stress model in mice. J. Neuroinflammation *13*, 108.

Cryan, J.F., and Dinan, T.G. (2012). Mind-altering microorganisms: the impact of the gut microbiota on brain and behaviour. Nat. Rev. Neurosci. *13*, 701–712.

De Palma, G., Lynch, M.D.J., Lu, J., Dang, V.T., Deng, Y., Jury, J., Umeh, G., Miranda, P.M., Pigrau Pastor, M., Sidani, S., et al. (2017). Transplantation of fecal microbiota from patients with irritable bowel syndrome alters gut function and behavior in recipient mice. Sci. Transl. Med. *9*, 9.

De Preter, V., Van Staeyen, G., Esser, D., Rutgeerts, P., and Verbeke, K. (2009). Development of a screening method to determine the pattern of fermentation metabolites in faecal samples using on-line purge-and-trap gas chromatographic-mass spectrometric analysis. J. Chromatogr. A *1216*, 1476–1483.

De Santis, S., Bach, P., Pérez-Cervera, L., Cosa-Linan, A., Weil, G., Vollstädt-Klein, S., Hermann, D., Kiefer, F., Kirsch, P., Ciccocioppo, R., et al. (2019). Microstructural white matter alterations in men with alcohol use disorder and rats with excessive alcohol consumption during early abstinence. JAMA Psychiatry *76*, 749–758.

de Timary, P., Cordovil de Sousa Uva, M., Denoël, C., Hebborn, L., Derely, M., Desseilles, M., and Luminet, O. (2013). The associations between self-consciousness, depressive state and craving to drink among alcohol dependent patients undergoing protracted withdrawal. PLoS ONE *8*, e71560.

Deaciuc, I.V., Arteel, G.E., Peng, X., Hill, D.B., and McClain, C.J. (2004). Gene expression in the liver of rats fed alcohol by means of intragastric infusion. Alcohol *33*, 17–30.

Dencker, D., Molander, A., Thomsen, M., Schlumberger, C., Wortwein, G., Weikop, P., Benveniste, H., Volkow, N.D., and Fink-Jensen, A. (2018). Ketogenic diet suppresses alcohol withdrawal syndrome in rats. Alcohol. Clin. Exp. Res. *42*, 270–277.

Derr, R.F., Draves, K., and Derr, M. (1983). Suppression of an ethanol withdrawal syndrome in rats by butyrate, lactate and β-hydroxybutyrate. Life Sci. *32*, 2551–2554.

Desbonnet, L., Clarke, G., Shanahan, F., Dinan, T.G., and Cryan, J.F. (2014). Microbiota is essential for social development in the mouse. Mol. Psychiatry *19*, 146–148.

Diaz Heijtz, R., Wang, S., Anuar, F., Qian, Y., Björkholm, B., Samuelsson, A., Hibberd, M.L., Forssberg, H., and Pettersson, S. (2011). Normal gut microbiota modulates brain development and behavior. Proc. Natl. Acad. Sci. USA *108*, 3047–3052.

di Penta, A., Moreno, B., Reix, S., Fernandez-Diez, B., Villanueva, M., Errea, O., Escala, N., Vandenbroeck, K., Comella, J.X., and Villoslada, P. (2013). Oxidative stress and proinflammatory cytokines contribute to demyelination and axonal damage in a cerebellar culture model of neuroinflammation. PLoS ONE *8*, e54722.

Dubinkina, V.B., Tyakht, A.V., Odintsova, V.Y., Yarygin, K.S., Kovarsky, B.A., Pavlenko, A.V., Ischenko, D.S., Popenko, A.S., Alexeev, D.G., Taraskina, A.Y., et al. (2017). Links of gut microbiota composition with alcohol dependence syndrome and alcoholic liver disease. Microbiome *5*, 141.

Edgar, R.C. (2013). UPARSE: highly accurate OTU sequences from microbial amplicon reads. Nat. Methods *10*, 996–998.

Eren, A.M., Vineis, J.H., Morrison, H.G., and Sogin, M.L. (2013). A filtering method to generate high quality short reads using Illumina paired-end technology. PLoS ONE *8*, e66643.

Erickson, E.K., Grantham, E.K., Warden, A.S., and Harris, R.A. (2019). Neuroimmune signaling in alcohol use disorder. Pharmacol. Biochem. Behav. *177*, 34–60.

Forsythe, P., Kunze, W., and Bienenstock, J. (2016). Moody microbes or fecal phrenology: what do we know about the microbiota-gut-brain axis? BMC Med. *14*, 58.

Fu, S.-P., Wang, J.-F., Xue, W.-J., Liu, H.-M., Liu, B.R., Zeng, Y.-L., Li, S.-N., Huang, B.-X., Lv, Q.-K., Wang, W., and Liu, J.X. (2015). Anti-inflammatory effects of BHBA in both in vivo and in vitro Parkinson's disease models are mediated by GPR109A-dependent mechanisms. J. Neuroinflammation *12*, 9.

Gacias, M., Gaspari, S., Santos, P.-M.G., Tamburini, S., Andrade, M., Zhang, F., Shen, N., Tolstikov, V., Kiebish, M.A., Dupree, J.L., et al. (2016). Microbiota-driven transcriptional changes in prefrontal cortex override genetic differences in social behavior. eLife *5*, 5.

Galli, A., Pinaire, J., Fischer, M., Dorris, R., and Crabb, D.W. (2001). The transcriptional and DNA binding activity of peroxisome proliferator-activated receptor alpha is inhibited by ethanol metabolism. A novel mechanism for the development of ethanol-induced fatty liver. J. Biol. Chem. *276*, 68–75.

Gilpin, N.W., and Koob, G.F. (2008). Neurobiology of alcohol dependence: focus on motivational mechanisms. Alcohol Res. Health *31*, 185–195.

Grabacka, M., Pierzchalska, M., Dean, M., and Reiss, K. (2016). Regulation of ketone body metabolism and the role of PPARα. Int. J. Mol. Sci. *17*, 27983603.

He, J., and Crews, F.T. (2008). Increased MCP-1 and microglia in various regions of the human alcoholic brain. Exp. Neurol. *210*, 349–358.

Herman, J.P., Mueller, N.K., and Figueiredo, H. (2004). Role of GABA and glutamate circuitry in hypothalamo-pituitary-adrenocortical stress integration. Ann. N Y Acad. Sci. *1018*, 35–45.

Hsiao, E.Y., McBride, S.W., Hsien, S., Sharon, G., Hyde, E.R., McCue, T., Codelli, J.A., Chow, J., Reisman, S.E., Petrosino, J.F., et al. (2013). Microbiota modulate behavioral and physiological abnormalities associated with neurodevelopmental disorders. Cell *155*, 1451–1463.

Hulse, R.E., Kunkler, P.E., Fedynyshyn, J.P., and Kraig, R.P. (2004). Optimization of multiplexed bead-based cytokine immunoassays for rat serum and brain tissue. J. Neurosci. Methods *136*, 87–98.

Jadhav, K.S., Peterson, V.L., Halfon, O., Ahern, G., Fouhy, F., Stanton, C., Dinan, T.G., Cryan, J.F., and Boutrel, B. (2018). Gut microbiome correlates with altered striatal dopamine receptor expression in a model of compulsive alcohol seeking. Neuropharmacology *141*, 249–259.

Janik, R., Thomason, L.A.M., Stanisz, A.M., Forsythe, P., Bienenstock, J., and Stanisz, G.J. (2016). Magnetic resonance spectroscopy reveals oral Lactobacillus promotion of increases in brain GABA, N-acetyl aspartate and glutamate. Neuroimage *125*, 988–995.

Jonas, D.E., Amick, H.R., Feltner, C., Bobashev, G., Thomas, K., Wines, R., Kim, M.M., Shanahan, E., Gass, C.E., Rowe, C.J., and Garbutt, J.C. (2014). Pharmacotherapy for adults with alcohol use disorders in outpatient settings: a systematic review and meta-analysis. JAMA *311*, 1889–1900.

Koper, J.W., Lopes-Cardozo, M., and Van Golde, L.M. (1981). Preferential utilization of ketone bodies for the synthesis of myelin cholesterol in vivo. Biochim. Biophys. Acta *666*, 411–417.

Le Roy, T., Debédat, J., Marquet, F., Da-Cunha, C., Ichou, F., Guerre-Millo, M., Kapel, N., Aron-Wisnewsky, J., and Clément, K. (2019). Comparative evaluation of microbiota engraftment following fecal microbiota transfer in mice models: age, kinetic and microbial status matter. Front. Microbiol. *9*, 3289.

Leclercq, S., Cani, P.D., Neyrinck, A.M., Stärkel, P., Jamar, F., Mikolajczak, M., Delzenne, N.M., and de Timary, P. (2012). Role of intestinal permeability and inflammation in the biological and behavioral control of alcohol-dependent subjects. Brain Behav. Immun. *26*, 911–918.

Leclercq, S., Matamoros, S., Cani, P.D., Neyrinck, A.M., Jamar, F., Stärkel, P., Windey, K., Tremaroli, V., Bäckhed, F., Verbeke, K., et al. (2014). Intestinal permeability, gut-bacterial dysbiosis, and behavioral markers of alcohol-dependence severity. Proc. Natl. Acad. Sci. USA *111*, E4485–E4493.

Lewohl, J.M., Wang, L., Miles, M.F., Zhang, L., Dodd, P.R., and Harris, R.A. (2000). Gene expression in human alcoholism: microarray analysis of frontal cortex. Alcohol. Clin. Exp. Res. *24*, 1873–1882.

Lippai, D., Bala, S., Petrasek, J., Csak, T., Levin, I., Kurt-Jones, E.A., and Szabo, G. (2013). Alcohol-induced IL-1β in the brain is mediated by NLRP3/ASC inflammasome activation that amplifies neuroinflammation. J. Leukoc. Biol. *94*, 171–182.

Liu, J., Dietz, K., DeLoyht, J.M., Pedre, X., Kelkar, D., Kaur, J., Vialou, V., Lobo, M.K., Dietz, D.M., Nestler, E.J., et al. (2012). Impaired adult myelination in the prefrontal cortex of socially isolated mice. Nat. Neurosci. *15*, 1621–1623.

Liu, J., Dupree, J.L., Gacias, M., Frawley, R., Sikder, T., Naik, P., and Casaccia, P. (2016). Clemastine enhances myelination in the prefrontal cortex and rescues behavioral changes in socially isolated mice. J. Neurosci. *36*, 957–962.

Manglani, M., Rua, R., Hendricksen, A., Braunschweig, D., Gao, Q., Tan, W., Houser, B., McGavern, D.B., and Oh, K. (2019). Method to quantify cytokines and chemokines in mouse brain tissue using Bio-Plex multiplex immunoassays. Methods Adv. Bead-Based Biomark. Detect. *158*, 22–26.

Mattson, M.P., Moehl, K., Ghena, N., Schmaedick, M., and Cheng, A. (2018). Intermittent metabolic switching, neuroplasticity and brain health. Nat. Rev. Neurosci. *19*, 63–80.

Maurage, P., Joassin, F., Philippot, P., Heeren, A., Vermeulen, N., Mahau, P., Delperdange, C., Corneille, O., Luminet, O., and de Timary, P. (2012). Disrupted regulation of social exclusion in alcohol-dependence: an fMRI study. Neuropsychopharmacology *37*, 2067–2075.

Maurage, F., de Timary, P., Tecco, J.M., Lechantre, S., and Samson, D. (2015). Theory of mind difficulties in patients with alcohol dependence: beyond the prefrontal cortex dysfunction hypothesis. Alcohol. Clin. Exp. Res. *39*, 980–988.

McNally, M.A., and Hartman, A.L. (2012). Ketone bodies in epilepsy. J. Neurochem. *121*, 28–35.

Mikolajczak, M., Luminet, O., Leroy, C., and Roy, E. (2007). Psychometric properties of the Trait Emotional Intelligence Questionnaire: factor structure, reliability, construct, and incremental validity in a French-speaking population. J. Pers. Assess. *88*, 338–353.

Moreira, T.J., Pierre, K., Maekawa, F., Repond, C., Cebere, A., Liljequist, S., and Pellerin, L. (2009). Enhanced cerebral expression of MCT1 and MCT2 in a rat ischemia model occurs in activated microglial cells. J. Cereb. Blood Flow Metab. *29*, 1273–1283.

Mutlu, E.A., Gillevet, P.M., Rangwala, H., Sikaroodi, M., Naqvi, A., Engen, P.A., Kwasny, M., Lau, C.K., and Keshavarzian, A. (2012). Colonic microbiome is

altered in alcoholism. Am. J. Physiol. Gastrointest. Liver Physiol. *302*, G966–G978.

Neufeld, K.M., Kang, N., Bienenstock, J., and Foster, J.A. (2011). Reduced anxiety-like behavior and central neurochemical change in germ-free mice. Neurogastroenterol. Motil. Off. J. Eur. Gastrointest. Motil. Soc. *23*, 255–264, e119.

Nguyen, T.L.A., Vieira-Silva, S., Liston, A., and Raes, J. (2015). How informative is the mouse for human gut microbiota research? Dis. Model. Mech. *8*, 1–16.

Olmos, G., and Lladó, J. (2014). Tumor necrosis factor alpha: a link between neuroinflammation and excitotoxicity. Mediators Inflamm. *2014*, 861231.

Parlee, S.D., Lentz, S.I., Mori, H., and MacDougald, O.A. (2014). Quantifying size and number of adipocytes in adipose tissue. Methods Enzymol. *537*, 93–122.

Pascual, M., Baliño, P., Aragón, C.M.G., and Guerri, C. (2015). Cytokines and chemokines as biomarkers of ethanol-induced neuroinflammation and anxiety-related behavior: role of TLR4 and TLR2. Neuropharmacology *89*, 352–359.

Pelletier, L.G., and Vallerand, R.J. (1990). L'échelle révisée de conscience de soi: une traduction et une validation Canadienne-Française du revised Self-Consciousness Scale. Can. J. Behav. Sci. Rev. Can. Sci. Comport. *22*, 191–206.

Peterson, V.L., Jury, N.J., Cabrera-Rubio, R., Draper, L.A., Crispie, F., Cotter, P.D., Dinan, T.G., Holmes, A., and Cryan, J.F. (2017). Drunk bugs: chronic vapour alcohol exposure induces marked changes in the gut microbiome in mice. Behav. Brain Res. *323*, 172–176.

Petrides, K.V., and Furnham, A. (2003). Trait emotional intelligence: behavioural validation in two studies of emotion recognition and reactivity to mood induction. Eur. J. Pers. *17*, 39–57.

Pfefferbaum, A., Adalsteinsson, E., and Sullivan, E.V. (2006). Dysmorphology and microstructural degradation of the corpus callosum: interaction of age and alcoholism. Neurobiol. Aging *27*, 994–1009.

Pfefferbaum, A., Rosenbloom, M., Rohlfing, T., and Sullivan, E.V. (2009). Degradation of association and projection white matter systems in alcoholism detected with quantitative fiber tracking. Biol. Psychiatry *65*, 680–690.

Puchalska, P., and Crawford, P.A. (2017). Multi-dimensional roles of ketone bodies in fuel metabolism, signaling, and therapeutics. Cell Metab. *25*, 262–284.

Rahman, M., Muhammad, S., Khan, M.A., Chen, H., Ridder, D.A., Müller-Fielitz, H., Pokorná, B., Vollbrandt, T., Stölting, I., Nadrowitz, R., et al. (2014). The β-hydroxybutyrate receptor HCA_2 activates a neuroprotective subset of macrophages. Nat. Commun. *5*, 3944.

Reikvam, D.H., Erofeev, A., Sandvik, A., Grcic, V., Jahnsen, F.L., Gaustad, P., McCoy, K.D., Macpherson, A.J., Meza-Zepeda, L.A., and Johansen, F.-E. (2011). Depletion of murine intestinal microbiota: effects on gut mucosa and epithelial gene expression. PLoS ONE *6*, e17996.

Richard, V., Conotte, R., Mayne, D., and Colet, J.-M. (2017). Does the 1H-NMR plasma metabolome reflect the host-tumor interactions in human breast cancer? Oncotarget *8*, 49915–49930.

Ridaura, V.K., Faith, J.J., Rey, F.E., Cheng, J., Duncan, A.E., Kau, A.L., Griffin, N.W., Lombard, V., Henrissat, B., Bain, J.R., et al. (2013). Gut microbiota from twins discordant for obesity modulate metabolism in mice. Science *341*, 1241214.

Rolland, J., and Mogelet, J. (2001). Manuel du système D5D.

Samuelson, D.R., Gu, M., Shellito, J.E., Molina, P.E., Taylor, C.M., Luo, M., and Welsh, D.A. (2019). Intestinal microbial products from alcohol-fed mice contribute to intestinal permeability and peripheral immune activation. Alcohol. Clin. Exp. Res. *43*, 2122–2133.

Sarkola, T., and Eriksson, C.J. (2001). Effect of 4-methylpyrazole on endogenous plasma ethanol and methanol levels in humans. Alcohol. Clin. Exp. Res. *25*, 513–516.

Scheier, M.F., and Carver, C.S. (1985). The Self-Consciousness Scale: a revised version for use with general populations. J. Appl. Soc. Psychol. *15*, 687–699.

Schloss, P.D., Westcott, S.L., Ryabin, T., Hall, J.R., Hartmann, M., Hollister, E.B., Lesniewski, R.A., Oakley, B.B., Parks, D.H., Robinson, C.J., et al. (2009). Introducing mothur: open-source, platform-independent, community-supported software for describing and comparing microbial communities. Appl. Environ. Microbiol. *75*, 7537–7541.

Sharon, G., Cruz, N.J., Kang, D.-W., Gandal, M.J., Wang, B., Kim, Y.-M., Zink, E.M., Casey, C.P., Taylor, B.C., Lane, C.J., et al. (2019). Human gut microbiota from autism spectrum disorder promote behavioral symptoms in mice. Cell *177*, 1600–1618.e17.

Sherwin, E., Bordenstein, S.R., Quinn, J.L., Dinan, T.G., and Cryan, J.F. (2019). Microbiota and the social brain. Science *366*, eaar2016.

Sidor, M.M., Rilett, K., and Foster, J.A. (2010). Validation of an automated system for measuring anxiety-related behaviours in the elevated plus maze. J. Neurosci. Methods *188*, 7–13.

Sokol, H., Pigneur, B., Watterlot, L., Lakhdari, O., Bermúdez-Humarán, L.G., Gratadoux, J.J., Blugeon, S., Bridonneau, C., Furet, J.P., Corthier, G., et al. (2008). *Faecalibacterium prausnitzii* is an anti-inflammatory commensal bacterium identified by gut microbiota analysis of Crohn disease patients. Proc. Natl. Acad. Sci. USA *105*, 16731–16736.

Stumpf, S.K., Berghoff, S.A., Trevisiol, A., Spieth, L., Düking, T., Schneider, L.V., Schlaphoff, L., Dreha-Kulaczewski, S., Bley, A., Burfeind, D., et al. (2019). Ketogenic diet ameliorates axonal defects and promotes myelination in Pelizaeus-Merzbacher disease. Acta Neuropathol. *138*, 147–161.

Valenta, J.P., and Gonzales, R.A. (2016). Chronic intracerebroventricular infusion of monocyte chemoattractant protein-1 leads to a persistent increase in sweetened ethanol consumption during operant self-administration but does not influence sucrose consumption in Long-Evans rats. Alcohol. Clin. Exp. Res. *40*, 187–195.

Walter, J., Armet, A.M., Finlay, B.B., and Shanahan, F. (2020). Establishing or exaggerating causality for the gut microbiome: lessons from human microbiota-associated rodents. Cell *180*, 221–232.

Wang, G., Liu, Q., Guo, L., Zeng, H., Ding, C., Zhang, W., Xu, D., Wang, X., Qiu, J., Dong, Q., et al. (2018). Gut microbiota and relevant metabolites analysis in alcohol dependent mice. Front. Microbiol. *9*, 1874.

Webber, R.J., and Edmond, J. (1979). The in vivo utilization of acetoacetate, D-(-)-3-hydroxybutyrate, and glucose for lipid synthesis in brain in the 18-day-old rat. Evidence for an acetyl-CoA bypass for sterol synthesis. J. Biol. Chem. *254*, 3912–3920.

Wiegel, J., Tanner, R., and Rainey, F.A. (2006). An introduction to the family Clostridiaceae. The Prokaryotes, Volume 4. Bacteria: Firmicutes Cyanobacteria (Springer Nature), pp. 654–678.

Wrzosek, L., Ciocan, D., Borentain, P., Spatz, M., Puchois, V., Hugot, C., Ferrere, G., Mayeur, C., Perlemuter, G., and Cassard, A.-M. (2018). Transplantation of human microbiota into conventional mice durably reshapes the gut microbiota. Sci. Rep. *8*, 6854.

Yang, M., Silverman, J.L., and Crawley, J.N. (2011). Automated three-chambered social approach task for mice. Curr. Protoc. Neurosci. *Chapter 8*, Unit 8.26.

Yeh, P.-H., Simpson, K., Durazzo, T.C., Gazdzinski, S., and Meyerhoff, D.J. (2009). Tract-Based Spatial Statistics (TBSS) of diffusion tensor imaging data in alcohol dependence: abnormalities of the motivational neurocircuitry. Psychiatry Res. *173*, 22–30.

Yuan, J., Chen, C., Cui, J., Lu, J., Yan, C., Wei, X., Zhao, X., Li, N., Li, S., Xue, G., et al. (2019). Fatty liver disease caused by high-alcohol-producing *Klebsiella pneumoniae*. Cell Metab., P675–P688.e7. 4.

Zhang, H., Sparks, J.B., Karyala, S.V., Settlage, R., and Luo, X.M. (2015). Host adaptive immunity alters gut microbiota. ISME J. *9*, 770–781.

Zhang, X., Yasuda, K., Gilmore, R.A., Westmoreland, S.V., Platt, D.M., Miller, G.M., and Vallender, E.J. (2019). Alcohol-induced changes in the gut

microbiome and metabolome of rhesus macaques. Psychopharmacology (Berl.) *236*, 1531–1544.

Zhao, W., Hu, Y., Li, C., Li, N., Zhu, S., Tan, X., Li, M., Zhang, Y., Xu, Z., Ding, Z., et al. (2020). Transplantation of fecal microbiota from patients with alcoholism induces anxiety/depression behaviors and decreases brain mGluR1/PKC ε levels in mouse. Biofactors *46*, 38–54.

Zheng, P., Zeng, B., Zhou, C., Liu, M., Fang, Z., Xu, X., Zeng, L., Chen, J., Fan, S., Du, X., et al. (2016). Gut microbiome remodeling induces depressive-like behaviors through a pathway mediated by the host's metabolism. Mol. Psychiatry *21*, 786–796.

Zywiak, W.H., Westerberg, V.S., Connors, G.J., and Maisto, S.A. (2003). Exploratory findings from the Reasons for Drinking Questionnaire. J. Subst. Abuse Treat. *25*, 287–292.

STAR★METHODS

KEY RESOURCES TABLE

REAGENT or RESOURCE	SOURCE	IDENTIFIER
Antibodies		
PSD95 (D27E11) XP® Rabbit mAb	Cell signaling	Cat#3450; RRID:AB_2292883
GAPDH (D16H11) XP® Rabbit mAb	Cell signaling	Cat#5174; RRID:AB_10622025
Goat Anti-Rabbit IgG Antibody, Peroxidase Conjugated	Merck Millipore	Cat# AP132P; RRID:AB_90264
Chemicals, Peptides, and Recombinant Proteins		
Ampicillin sodium salt	SIGMA-ALDRICH	CAS Number: 69-52-3
Neomycin	SIGMA-ALDRICH	CAS Number: 1405-10-3
Metronidazole	SIGMA-ALDRICH	CAS Number: 443-48-1
Amphotericin B solubilized	SIGMA-ALDRICH	CAS Number:1397-89-3
Vancomycin hydrochloride	VWR	CAS Number: 1404-93-9
LPS *Escherichia coli* 0111: B4	SIGMA-ALDRICH	Cat# LPS25
Critical Commercial Assays		
QIAamp DNA Stool Mini Kit	QIAGEN	Cat# 51504
Mouse Bio-Plex Pro Assays	Biorad	Customized
Corticosterone ELISA kit	Enzo Life Sciences	Cat# ADI-900-097
GABA ELISA	ImmuSmol	Cat# BA E-2500
Glutamate ELISA	ImmuSmol	Cat# BA E-2400
Beta-hydroxybutyrate assay kit	Abcam	Cat# ab83390
Non-esterified fatty acids assay	Randox	Cat# FA115
Ethanol Colorimetric/Fluorometric Assay Kit	Biovision	Cat# K620-100
Deposited Data		
Raw data generated with the 16S rRNA gene sequencing	SRA	BioProject PRJNA553184
Experimental Models: Organisms/Strains		
Mouse C57BL/6J, specific pathogen-free (male)	Janvier Labs	N/A
Oligonucleotides		
Primer sequences used for RT-qPCR	See Table S3	N/A
Software and Algorithms		
SPSS 25.0	IBM	N/A
R 3.4.2	Cran R project, https://cran.r-project.org/bin/windows/base/old/3.4.2/	N/A
USEARCH v10.02.240	Edgar, 2013	N/A
Mothur v.1.25.0	Schloss et al., 2009	N/A
BrainVoyager 20.6	Brain Innovation	N/A
MestReNova 10.0.2	Mestrelab Research	N/A
SIMCA-P+12.0	Umetrics	N/A
EthoVision XT software V14	Noldus	N/A
Leica Image Viewer Software 4.0.7	Leica Microsystems	N/A
ImageJ	NIH, https://imagej.nih.gov/ij/download.html	N/A
ImageQuantTL 8.2	GE Heathcare	N/A
MetaboAnalyst V4.0	MetaboAnalyst, https://www.metaboanalyst.ca/	N/A
GraphPad Prism 7	GraphPad Prism	N/A

RESOURCE AVAILABILITY

Lead Contact

Further information and requests for resources and reagents should be directed to and will be fulfilled by the Lead Contact, Nathalie Delzenne (nathalie.delzenne@uclouvain.be).

Materials Availability

This study did not generate new unique reagents.

Data and Code Availability

The accession number for the raw data generated with the 16S rRNA gene sequencing reported in this paper is BioProject PRJNA553184 (SRA).

EXPERIMENTAL MODEL AND SUBJECT DETAILS

For human studies

Recruitment of alcohol-dependent subjects and healthy controls

The population of patients and controls displayed in Figure 1 belong to the same cohort as that recruited for our previous publication (Leclercq et al., 2014). Because they were recruited before the publication of Diagnostic and Statistical Manual of Mental Disorders (DSM) 5 criteria, they were diagnosed by psychiatric evaluation (P.d.T) as alcohol-dependent (AD) according to the DSM-IV criteria, and did not present with other major psychiatric comorbidities. Among those participants, 2 AD patients and 2 CT subjects were selected as donors for the FMT experiment. They were all psychoactive drugs-free. Their age, sex, biological and psychological features are described in Table S2. Patients displayed in Figure 7 belong to more recent cohorts and were diagnosed as severe AUD using DSM 5 criteria (mean age (y): 48 ± 10 [min: 27, max: 71], 67% males and 33% females). Exclusion criteria are similar for all cohorts. Patients suffering from metabolic disorders such as obesity [body mass index (BMI) > 30 kg/m^2] and diabetes, inflammatory bowel disease, other chronic inflammatory diseases (such as rheumatoid arthritis), or cancer, as well as those who had taken antibiotics, probiotics, glucocorticoids, or nonsteroidal anti-inflammatory drugs during the 2 months preceding enrollment were excluded from the study. Patients enrolled in this study were admitted to the gastroenterology ward for a 3-week detoxification and rehabilitation program in St Luc academic hospital (Brussels, Belgium) and received benzodiazepines as a standard treatment to manage the withdrawal symptoms during the first week of hospitalization only. The control group (CT) consists in age-, sex- and BMI-matched healthy subjects who consumed less than 20 g of alcohol per day. The protocol related to the clinical study was approved by the local ethical committee (commission d'éthique biomédicale hospitalo-facultaire de l'Université catholique de Louvain) and all subjects signed an informed consent form before the investigation (B40320096274; 2009/17AVR/140 with amendment 27/02/2017, and 2014/31DEC/614).

For in vivo animal studies

All animal experiments were approved by and performed in accordance with the guidelines of the ethics committee of the Université catholique de Louvain under the specific agreement number 2017/UCL/MD/005. Housing conditions were as specified by the Belgian Law of 23 May 2013, on the protection of laboratory animals (Agreement LA 1230314).

Mice used for FMT experiment

Three-week old specific pathogen-free (SPF) C57BL/6J male mice (n = 24) were obtained from Janvier Labs (France). Mice were randomly assigned to experimental groups (CT-recipient and AD-recipient) and were housed in groups of three in individually ventilated cages (IVC) on a 12-hour daylight cycle with *ad libitum* access to sterile water and gamma-irradiated standard chow diet (AIN-93M, Research Diets, NJ, USA). Mice were systematically handled under a laminar flow cabinet and gloves were changed between each group handling. Body weight, food and water intake were daily measured during the antibiotic treatment. Feces were collected at three time points (23, 35 and 45 days after FMT) in order to study the kinetics of the microbial taxa engraftment in mice transplanted with human fecal samples.

Mice used for the ketogenic diet experiment

Seven-week old specific pathogen-free (SPF) C57BL/6J male mice were obtained from Janvier Labs (France). Mice were randomly assigned to experimental groups (CT and KD). Mice were housed in groups of three in individually ventilated cages (IVC) on a 12-hour daylight cycle with *ad libitum* access to sterile water and gamma-irradiated standard chow diet (AIN-93M, Research Diets, NJ, USA) (CT group, n = 21) or ketogenic diet (80% fat, Ssniff, Germany) (KD group, n = 21) for 6 weeks. Mice of the KD group have been submitted to a keto-adaptation during 2 weeks. The ketogenic diet has been mixed to chow diet in the following proportion: 50% KD during 3 days, 70% KD for 4 days, 90% KD for 7 days. For 9 mice per group, intraperitoneal injection of low dose LPS (100μg/kg, *Escherichia coli* 0111: B4, Sigma-Aldrich) have been performed 24h before necropsy to induce a neuroinflammation, as described previously (Couch et al., 2016).

METHOD DETAILS

Psychological questionnaires

Self-reported psychological questionnaires, i.e., the State-trait Anxiety (STAI), the Beck Depression Inventory (BDI), and the Obsessive Compulsive Drinking Scale (OCDS) were used to assess anxiety, depression and alcohol craving as described previously (Leclercq et al., 2012). Several questionnaires were also administered to assess different personality dimensions. First, trait emotional intelligence (EI) was measured through a self-reported questionnaire that consists in 75 items rated on a 7-point scale. It assesses a global trait EI score as well as scores on 4 specific factors: well-being, self-control, emotionality and sociability. The psychometric properties of the French version have been validated (Mikolajczak et al., 2007). Second, we used the Description in Five Dimension system of personality (D5D) (Rolland and Mogelet, 2001), which is based on the Big Five model and evaluates five dimensions, namely emotional stability, introversion, openness, conscientiousness and agreeableness, through 55 adjectives rated along a 6-point scale. The sociability factor of EI and introversion scale of D5D have been shown to be correlated (Mikolajczak et al., 2007). Finally, the French version of the Revised Self-Consciousness scale (RSCS) was used to assess individual levels of trait self-consciousness (SC), which is a personality trait characterized by a tendency to think and to direct attention toward the self (Pelletier and Vallerand, 1990; Scheier and Carver, 1985), an important dimension of alcohol dependence (de Timary et al., 2013). This scale includes 22 items and contains three main separate facets of SC which are private SC, public SC and social anxiety. This latter facet questions another facet of sociability difficulties as it reflects the extent to which individuals focus on themselves when experiencing discomfort in front of others.

Intestinal permeability and gut microbiota composition measurements in humans

Intestinal permeability was assessed using the ^{51}Cr-EDTA method, with 24h-urine collection as described in our previous study (Leclercq et al., 2014). Leaky gut (high intestinal permeability) was calculated according to a deviance criterion at a threshold of 1.65 SDs of the mean of the control group as explained in details in our previous publication (Leclercq et al., 2014). Gut microbiota composition was evaluated in the fecal samples by 16S rDNA sequencing and qPCR as described in our previous study (Leclercq et al., 2014).

Ethanol measurement in human fecal samples by GC/MS

A detailed description of the method has already been published previously (De Preter et al., 2009; Leclercq et al., 2014). Briefly, VOCs in fecal sample were analyzed on a gas chromatography-mass spectrometry quadrupole (Trace GC, Thermoquest; DSQ II, Thermo Electron), which was coupled online to a purge-and-trap system (SOLAtek 72 and Velocity XPT, Teledyne Tekmar, Mason, OH, USA). Before analysis, 125-mg fecal aliquots were suspended in 5 mL of water. Diethyl acetic acid (1.5 mg/L) was added as an internal standard. A magnetic stirrer, sulfuric acid, and a pinch of sodium sulfate were added to the sample to acidify and salt out the solution. The chromatograms thus obtained were processed by using AMDIS (Automatic Mass Spectral Deconvolution and Identification Software, version 2.71) provided by the US National Institute of Standards and Technology (NIST). Ethanol was then relatively quantified compared with diethyl acetic acid.

Neuroimaging assessment

Data acquisition

At the end of a 3-week detoxification program, 22 alcohol-dependent patients (mean age: 47 ± 11; 13 men, 9 women) underwent MRI scanning (3D T1 and DTI) using a 3T Achieva (Philips Healthcare, Eindhoven, the Netherlands), equipped with a 32-channel phased array head coil. The anatomical 3D sequence consisted of a gradient-echo sequence with an inversion prepulse (Turbo Field Echo, TFE) acquired in the sagittal plane using the following parameters: repetition time (TR) = 9.1 ms, echo time (TE) = 4.6 ms, flip angle = 8°, number of slices = 150, slice thickness = 1 mm, in-plane resolution = 0.81 × 0.95 mm^2 (acquisition) reconstructed in 0.75 × 0.75 mm^2, field of view (FOV) = 220 × 197 mm^2, acquisition matrix = 296 × 247 (reconstruction 320^2), sensitivity encoding (SENSE) factor = 1.5 (parallel imaging). DTI images were acquired using the following sequence: spin-echo planar imaging, TE = 83 ms, TR = 6422 ms, Bandwidth = 2790hz/pixel, number of slices = 70, slice thickness = 2mm, in-plane resolution = 2 × 2 mm^2, matrix size = 112 × 112, FOV = 224 × 224 mm^2, 55 directions, b = 800 s/mm^2.

Data processing

Preprocessing of the DTI-data was performed using BrainVoyager (Version 20.6, Brain Innovation, Maastricht, the Netherlands). The diffusion data were first corrected for eddy current-induced distortions and motion-induced artifacts, and then coregistred to the 3D anatomy of the participants to create a volume diffusion weighted (vdw) data. All coregistrations were visually inspected, and possibly corrected manually if necessary. Fractional anisotropy (FA) maps were extracted from the vdw and normalized in Talairach space. Each subject's normalized map was then associated with the beta-hydroxybutyrate concentration to compute a correlation map on a voxel-based manner. The resulting map at $p < 0.05$ uncorrected was then corrected for multiple comparisons using cluster-size thresholding via MonteCarlo simulation (min size = 464 mm^3) and projected on the anatomical average of the 22 subjects. The two largest clusters were found in the white matter, one in the forceps major (size: 1893 mm^3, r = 0,656) and one in the left superior longitudinal fasciculus (size: 2155 mm^3, r = 0,757).

Antibiotic treatment and bowel cleansing procedure

Immediately after their arrival (Post-natal day (PND) 22), mice were administered broad-spectrum antibiotics cocktail (ampicillin, neomycin, metronidazole: 100mg/kg; vancomycin: 50mg/kg) by oral gavage once a day using flexible plastic feeding tubes (Instech Laboratories, the Netherlands) for 10 days. Amphothericin-B (1 mg/kg) was added to the antibiotic cocktail for the first 3 days to prevent fungi overgrowth. This antibiotic therapy has been previously shown to effectively deplete the intestinal microbiota while ensuring mice health (Reikvam et al., 2011). At the end of the antibiotic treatment, mice were subjected to intestinal purge with PEG 4000 (polytethylene glycol, macrogolum; 59 g/l supplemented with NaCl: 1.46 g/l; KCl: 0.75 g/l; Na_2SO_4: 5.68 g/l; $NaHCO_3$: 1.68 g/l)) in order to wash out the antibiotics remaining in the intestine. 1.5 mL of this intestinal bowel cleansing solution was administered by oral gavage to each mouse (2 X 500μL the day before FMT with 1 hour interval, and 1 X 500 μL 4h before the FMT). Mice were fasted 4 h before PEG administration. Since mice are coprophagous, the bedding was renewed after each intestinal purge.

Inoculum preparation

Human fecal samples were collected in sterile containers and stored immediately at −20°C and transferred for long-term storage at −80°C within 6 hours. Handling of human fecal samples was performed under anaerobic conditions (vinyl anaerobic chamber, Coy Lab, MI, USA). Each fecal sample (0.5 g) was suspended in 5 mL of reduced sterile PBS (0.05% L-cystein-HCL and N_2), then vortexed for 5 min followed by sedimentation for 5 min. The slurry was then passed through a 100 μM cell strainer and 200 μL of the suspension was immediately administered to the mice by oral gavage with flexible disposable plastic tubes. Aliquots of this suspension were frozen at −80°C with 10% glycerol for the next gavages.

Human microbiota transplantation into conventional mice

Fecal samples from 2 healthy controls (CT) and 2 alcohol-dependent (AD) patients with a well-characterized gut microbiota (Leclercq et al., 2014) were transferred to 24 mice (6 mice per donor, with a total of 12 AD-recipient and 12 CT-recipient mice). Microbial features of the donors are summarized in Table S2 and Figure S1. 200μL of inoculum were administered by oral gavage 4h after the third bowel cleansing procedure. Inoculum administration was repeated twice (2 days and 4 days after the first FMT) for a total of 3 FMT within the week. Mice were then allowed to rest for 2 weeks in the IVC cage with limited handling to ensure stable engraftment of the human microbiota.

Gut microbiota analysis

Genomic DNA was extracted from the mouse feces obtained at days 23, 35 and 45 post-FMT and caecal content obtained at necropsy using a QIAamp DNA Stool Mini Kit (QIAGEN, Germany), including a bead-beating step. The composition of the gut microbiota was analyzed by Illumina sequencing of the 16S rRNA gene, as previously described (Bindels et al., 2016). The V5-V6 region of the 16S rRNA gene was amplified by PCR with modified primers. The amplicons were purified, quantified and sequenced using an Illumina Miseq to produce 2x300-bp sequencing products at the University of Minnesota Genomics Center. Subsequent bioinformatics and biostatistics analyses were performed as previously described (Bindels et al., 2016). Initial quality-filtering of the reads was conducted with Illumina Software, yielding an average of 157737 pass-filter reads per sample. Quality scores were visualized, and reads were trimmed to 220 bp (R1) and 200 bp (R2). The reads were merged with the merge-Illumina-pairs application (Eren et al., 2013). For all samples but one, a subset of 25000 reads was randomly selected using Mothur v.1.25.0 (Schloss et al., 2009) to avoid large disparities in the number of sequences. Subsequently, the UPARSE pipeline implemented in USEARCH v10.02.240 (Edgar, 2013) was used to further process the sequences. Clustering was performed using the cluster_otus function which includes a chimera filtration, with 97% similarity cutoff to designate Operational Taxonomic Units (OTUs). Non-chimeric sequences were also subjected to taxonomic classification using the RDP MultiClassifier 1.1 from the Ribosomal Database Project (Cole et al., 2014) for phylum to genus characterization of the faecal and caecal microbiome. The phylotypes were computed as percent proportions based on the total number of sequences in each sample. Raw data generated with the 16S rRNA gene sequencing are available in SRA (BioProject PRJNA553184).

Metabolic profiling by ^{1}H-NMR spectroscopy

Blood samples from the 24 mice (6 mice per donor: 12 AD-recipient and 12 CT-recipient mice) were collected on EDTA tubes and the resulting plasma fractions were stored frozen at −80°C. To prepare samples for metabolomics analysis by ^{1}H-NMR spectroscopy, 70μl of plasma with 70μl D_2O (if insufficient plasma volume supplement with D_2O to obtain a total volume of 140 μl) were filtered using 3kDa Amicon® Ultra-0.5 mL Centrifugal Filter Devices (Millipore) at 14,000 x g during 15 minutes. The filter was initially prewashed four times with distilled water to remove any traces of preservatives. Then, 75μl of filtered plasma with 5μl of deutered 3-(trimethylsilyl) propionic-2,2,3,3-d4 acid (TSP) (0.25 mM final concentration) were transferred into the microcapillaire NMR tube and analyzed on a Bruker 600 spectrometer (14.1 T) at 600 MHz for proton observation within a 5 mm BBI 1H/D-probe. One-dimensional spectrum was acquired at 297° K using a NOESYPRESAT-1D pulse sequence using 256 free induction decays (FID). The FID signal was imported into MestReNova 10.0.2 Software (Mestrelab Research, Santiago de Compostela, Spain) for Fourier transform and a line broadening of 0.3 Hz was applied. Then the spectra were automatically phase and baseline-corrected and calibrated against TSP. The resonance of the methyl groups in TSP were arbitrarily placed at 0.00 ppm. Spectral region from 0.08 to 10.00 ppm was automatically reduced to 248 integrated regions (buckets) of 0.04 ppm width each. Regions from containing residual water signal (4.50 to 5.20ppm) and EDTA

resonances (3.20 to 3.22ppm and 3.58 to 3.62ppm) were excluded. Each integrated sub-region was then normalized to the total spectrum area. The final dataset was imported into SIMCA-P+12.0 software (Umetrics, Umea, Sweden). After pareto scaling, a partial least-squares discriminant analysis (PLS-DA) was performed. In the ''scores plot,'' each point corresponds to one observation, meaning the NMR spectrum of a sample (mouse). This simplified 2-D view of the dataset allows a quick identification of potential gathering or separation between AD-recipient and CT-recipient. The corresponding ''loadings plot'' highlights what variables (metabolites) are responsible for the discrimination of groups (each point corresponds to the mean chemical shift of a particular spectral sub-region of 0.04 ppm width and consequently to the corresponding plasma metabolites). These variables were finally annotated from an in-house database to identify the corresponding metabolites, as published previously (Richard et al., 2017).

Behavioral testing

Behavioral testing started 20 days after the first FMT. All behavioral tests were recorded by a video camera connected to a computer and data analysis was performed by using EthoVision XT software (Noldus, the Netherlands), except for the forced swim test which was assessed manually. Three sessions of animal handling were performed 1 week before the first behavioral test to reduce the level of stress induced by the experimenter. Mice were transported to the behavioral testing room for a 1h habituation period. All tests have been performed during the light phase. Each apparatus was thoroughly cleaned with water and dried between each animal. CT-recipient and AD-recipient mice were tested in a random order and allowed to rest for several days between each test. The experimenter was not blinded to the group allocation when performing the testing.

Light-dark box test

Mice were placed for 10 min in a clear Plexiglas enclosure containing a black insert on one side. Time spent and number of entries in the light zone were used to assess anxiety-like behavior (Bourin and Hascoët, 2003).

Elevated plus maze (EPM)

Mice were tested in the EPM apparatus which is elevated at 76 cm off the ground and consisting of 4 arms – 2 open arms and 2 closed arms made with black Plexiglas walls (Sidor et al., 2010). The mouse was placed in the intersection of the 4 arms, facing an open arm, and allowed to explore for 5 min. Time spent and number of entries in the open arms were used to assess anxiety-like behavior.

Three-chamber sociability test and preference for social novelty

The apparatus consists of 3 rectangular Plexiglas chambers whose dividing walls possess small openings that allow access into each chamber (Yang et al., 2011). The experimental mouse was first placed in the center chamber while the doorways were closed and allowed to explore for a 5-min habituation period. In the second phase of the test, an unfamiliar mouse (strain-, sex- and age-matched) was placed within an inverted wire cup in one of the outer chambers while an empty wire cup was placed in the other outer chamber. The doors to the outer chambers were opened and the sociability trial was conducted for 10 min during which the experimental mouse was allowed to explore the 3 chambers. Mouse and object chambers were virtually divided into 2 zones of equal size, and the zone containing the wire cup is defined as ''interaction zone.'' Time spent in each chamber/zone was recorded. Sociability is defined as the experimental mouse spending more time in the chamber containing the novel mouse than in the chamber containing the novel object. Sociability index is calculated as $[time_{mouse} / (time_{mouse} + time_{object})] \times 100$. In the third phase of the test, a second novel mouse (stranger 2) is placed inside the previously empty wire cup while the initial novel mouse (stranger 1) remains inside its cup. The experimental mouse is given 10min to explore all the three chambers. Preference for social novelty is defined as more time spent in the chamber with stranger 2 than time spent in the chamber with stranger 1.

Forced swim test

Mice were placed in an inescapable transparent Plexiglas tank (30 cm ×20 cm) fill with autoclaved water (15 cm from the bottom) at room temperature (Can et al., 2011). A video camera recorded each mouse for 6 minutes and manual scoring was performed by a trained experimenter who was blinded to the group allocation. Duration of immobility (during the 4 last minutes of the test) and latency to immobility were used to assess depression-like behavior. Water was renewed between each mouse. Before returning to their home cage, mice were gently dried with paper towels.

Blood and tissue sampling

Mice were anesthetized with isoflurane (Forene®, Abbott, England) and blood from portal vein and vena cava was centrifuged and serum/plasma samples were stored at −80°C until analysis. Mice were then killed by decapitation. Brain (frontal cortex, striatum and hippocampus) and gut (ileum) were carefully dissected and placed into RNAlater® solution (Life technologies) for RNA extraction. Tissues were incubated overnight at 4°C then transferred at −20°C until further processed. For brain protein extraction and for liver, tissues were dissected and immediately snap-frozen with liquid nitrogen then stored at −80°C. Histologic evaluation of villi height and crypt depth of the ileum and of adipocyte area of the subcutaneous adipose tissue, was performed in hematoxylin-eosin stained sections which were digitalized at a 20 × magnification using a SCN400 slide scanner (Leica, Wetzlar, Germany). Villi height and crypt depth were manually measured by an investigator blinded for group allocation using the Leica Image Viewer Software (Version 4.0.7; at least 10 measures of each parameter per section and two independent sections per mouse). Quantification of adipocyte size was calculated with ImageJ following the protocol of Parlee et al. (2014).

RNA extraction and RT-qPCR analysis

Following tissue homogenization with tissue lyzer (QIAGEN, Germany), total RNA was extracted using TRIzol® Reagent (Roche Diagnostic, Germany) according to the manufacturer's instructions. 1 μg RNA was then converted into cDNA using GoScript Reverse Transcriptase (Promega, Belgium). Diluted cDNA was used as template for qPCR reaction using SYBR Green MESA FAST qPCR MasterMix Plus for SYBR® Assay (Eurogentec, Belgium) for intestinal and liver samples analysis and Power SYBR®Green Master Mix (Applied Biosystem) containing ROX dye Passive Reference for brain samples analysis. The qPCR reactions were performed on QuanStudio3 machine (Applied Biosystem). All samples were run in duplicate and primers were used at a concentration of 300 nM. Data were normalized to the endogenous control gene RPL-19 and the relative quantification was analyzed using the ΔΔCt method. Primers were designed with Primer 3 and checked for specificity using Primer-BLAST. Primers were validated by performing a calibration curve using serial dilution of cDNA in the tissue of interest. Primers were considered acceptable when efficiency reaches 90% −110%. The purity of the amplified product was verified by analyzing the melt curve at the end of amplification. Primer sequences are listed in Table S3.

Protein extraction and western blot analysis

Brain tissues (frontal cortex) were quickly dissected following decapitation, immediately snap-frozen with liquid nitrogen then stored at −80°C. Samples were homogenized and lysed (45 min on ice) in RIPA protein lysis buffer (100 mL per 10 mg; 0.05M Tris-HCl, 0.15M Nacl, pH 7.4) containing 1% NP-40, 1mM EDTA, 10mM NaF, 0.5% sodium deoxycholate, 0.1% SDS, 1mM PMSF, 1mM Na3VO4 and protease inhibitor cocktail (1 tablet per 10 ml, cOmplete Roche, Sigma-Aldrich) and centrifuged at 12,000 g for 15 min at 4°C. The supernatant was collected and protein concentration was measured by the Lowry method (DC Protein Assay, Biorad). Proteins (10 μg) were fractionated on a 8% SDS–polyacrylamide gel electrophoresis gel and transferred to 0.2 mm polyvinylidene difluoride membranes (GE Healthcare Life Sciences, Germany). Membranes were blocked in 0.1% Tween-TBS 20 with 5% BSA for 1 h at room temperature, then probed with rabbit antibodies to PSD-95 (D27E11, Cell signaling, 1:1000, overnight, 4°C) or GAPDH (D16H11, Cell signaling, 1:5000, 2h, RT). After extensive washing, membranes were incubated for 1 h at room temperature with a goat anti-rabbit IgG-peroxidase secondary antibody (AP132P, Merck Millipore, 1:10000 for PSD-95 and 1:20000 for GAPDH detection) then visualized with ECL western blotting detection reagents (Super Signal West Pico Substrate, Thermo Scientific) and ImageQuantTL instrument and software 8.2 (GE Heathcare, Buckinghamshire, England). Densitometry was quantified with ImageJ.

Cytokines, corticosterone and ethanol assays

Serum samples obtained from portal vein and vena cava were used to measure inflammatory cytokines (Bio-Plex Pro, Biorad, Belgium), corticosterone (Enzo Life Sciences, Belgium) and ethanol (Biovision, Gentaur, Belgium) following manufacturer's instructions. Proteins were extracted from striatum by using the Bioplex Cell Lysis kit (Biorad, Belgium) and cytokines were measured using multiplex immuno assay with a protocol adapted from Hulse et al. (2004) and Manglani et al. (2019). Results were corrected for total protein concentration in the striatum.

GABA and glutamate ELISA

Neurotransmitters GABA and glutamate were measured by ELISA following manufacturer's instructions (ImmuSmol, France) and slightly adapted from the protocol of Janik et al. (2016). Brain lysates were diluted 1:10 and results were corrected for tissue weight.

Beta-hydroxybutyrate and non-esterified fatty acids assays

Blood sample have been collected from the mouse tail every two weeks to assess the kinetic of BHB levels upon ketogenic diet as well as in detoxified AD patients. BHB was measured in the serum following manufacturer's instructions (Abcam, UK). Dilutions were 1:10 for mouse serum and 1:2 for human samples. NEFA were measured following manufacturer's instructions (Randox, UK). Human and mouse samples were diluted 1:4.

QUANTIFICATION AND STATISTICAL ANALYSIS

All statistics were performed with SPSS 25.0 and R 3.4.2, and graphs were created with GraphPad Prism 7, Emperor (β diversity) and MetaboAnalyst V4.0. Assumptions of normality and equality of variances were checked with Kolmogorov-Smirnov and Levene tests, respectively. If the assumptions were met, unpaired t tests were used to compare alcohol-dependent patients versus controls subjects, AD-recipient versus CT-recipient mice and KD versus CT mice. If the assumptions were not met, non-parametric tests were used as specified in the figure legends. Results were considered statistically significant when $p < 0.05$ (two-tailed). For microbiota analysis, q value with FDR-correction was considered to compare the relative abundance of bacterial taxa in AD- and CT-recipient mice. Description of statistical tests used, number of patients/mice, mean and SD or SEM can be found in the figure legends.